world

MDPI

Article

Urban Heat Island and Environmental Degradation Analysis Utilizing a Remote Sensing Technique in Rapidly Urbanizing South Asian Cities

Md Tanvir Miah [1], Jannatun Nahar Fariha [1], Pankaj Kanti Jodder [2], Abdulla Al Kafy [3], Raiyan Raiyan [1], Salima Ahamed Usha [1], Juvair Hossan [4] and Khan Rubayet Rahaman [5,*]

[1] Urban and Rural Planning Discipline, Khulna University, Khulna 9208, Bangladesh; tanvir180417@gmail.com (M.T.M.); farihajannat720@gmail.com (J.N.F.); raiyanrockers@gmail.com (R.R.); ahamedusha.ku@gmail.com (S.A.U.)
[2] Department of Earth, Environmental and Geographical Sciences, University of North Carolina at Charlotte, Charlotte, NC 28213, USA; pankajkantijodder@gmail.com
[3] Department of Geography & the Environment, The University of Texas at Austin, Austin, TX 78712, USA; abdulla-al.kafy@localpathways.org
[4] Environmental Science Discipline, Khulna University, Khulna 9208, Bangladesh; juvairhossan181050@gmail.com
[5] Department of Geography and Environmental Studies, St. Mary's University, Halifax, NS B3H 3C3, Canada
* Correspondence: khan.rahaman@smu.ca

Abstract: Rapid urbanization in South Asian cities has triggered significant changes in land use and land cover (LULC), degrading natural biophysical components and intensifying urban heat islands (UHIs). This study investigated the impact of LULC changes on land surface temperature (LST) and the role of biophysical indicators in enhancing urban resilience to thermal extremes. We used Landsat satellite imageries from 1993 to 2023, conducted a comprehensive analysis of LULC changes, and estimated LST variations at 6-year intervals in the Dhaka, Gazipur, and Narayanganj districts in Bangladesh. Afterward, we performed statistical analysis upon employing correlation, regression, and principal component analysis (PCA) techniques to summarize information. The results reveal that 339.13 km^2 worth of urban expansion has occurred in last 30 years, with an average annual growth rate of 3.5%, accompanied by a substantial reduction in water bodies (−139.17 km^2) and vegetation cover. Consequently, summer temperatures exceeded approximately 36.52 °C in dense urban areas. Also, the results highlighted the strong influence of built-up areas (BSI and SAVI) on LST, while vegetation (NDVI) and water indices (NDWI) exhibited a negative association. The findings emphasize the urgency of integrating green infrastructure and deploying sustainable urban planning policies to mitigate the potential adverse impacts of scattered urbanization in the face of climate change.

Keywords: surface temperature; biophysical indicators; resilience; remote sensing; sustainable urban planning

Citation: Miah, M.T.; Fariha, J.N.; Jodder, P.K.; Al Kafy, A.; Raiyan, R.; Usha, S.A.; Hossan, J.; Rahaman, K.R. Urban Heat Island and Environmental Degradation Analysis Utilizing a Remote Sensing Technique in Rapidly Urbanizing South Asian Cities. *World* **2024**, *5*, 1023–1053. https://doi.org/10.3390/world5040052

Academic Editor: Mohammad Aslam Khan Khalil

Received: 16 September 2024
Revised: 23 October 2024
Accepted: 25 October 2024
Published: 29 October 2024

1. Introduction

Over the flow of time, the world has witnessed significant urban development, characterized by shifts in demographics, social dynamics, economic structures, and cultural norms, fundamentally altering the fabric of human existence [1]. Rapid urban expansion has triggered significant alterations of LULC, contributing to the rise of LST and reshaping local climate. Recently, there has been a clear indication of the changing biophysical composition in urban areas, largely influenced by temperature anomalies resulting from climate change [2–4]. This trend of shifting LST regimes tangibly impacts the strong connection between natural environment and urban ecosystem and damaging the biological systems and critical environmental components [5].

Interestingly, urbanization is significantly influencing both human livelihoods and demographic characteristics on a global scale. A recent assessment report from the United Nations has documented that over half of the world's population, accounting for approximately 55%, is currently living in urban areas [6]. This implies a notable change in the natural environment, leading to the transformation of aquatic ecosystems and shrub covers into resistant surfaces. This phenomenon highlights the significant impact of urban expansion on the ecological integrity and hydrological dynamics of natural environments and landscapes [7]. Consequently, this unforeseeable incidence exerts pressure on urban ecosystems, local climates, and energy flows, underscoring its multifaceted impact on environmental dynamics and urban sustainability [8]. From recent research [9,10], it has been clearly documented that rapid urban expansion has a significant impact on local and regional temperatures, along with the natural ecosystem (e.g., hydrology, vegetation, rainfall patterns, etc.). Scientists have explored the relationship between LULC and LST by performing various indices such as the normalized difference vegetation index (NDVI), normalized difference built-up index (NDBI), normalized difference bareness index (NDBAI), normalized difference water index (NDWI), and modified normalized difference water index (MNDWI) [11] to quantify the patterns and trends of shifts, and the way they amplify the impact of thermal islands in cities [11–13].

However, few studies have considered understanding the relationships between the LULC and biophysical environment in cities across the global south. Thus, it is important to study the complex relationships among LULC, LST, and biophysical factors concerning environmental resilience and sustainability for urban development. It should be noted that the search for the changing biophysical components and its contribution toward LST often remains overlooked, which is not only affected by the LULC, but also has a significant contribution in exacerbating the UHI effect, posing serious challenges for ecological sustainability and public health [7]. While existing literature delves into the association between the LULC and LST, there remains a vital need for addressing the role of natural components (e.g., NDVI and NDDWI). Therefore, it is imperative to comprehend the interrelationships between biophysical indices and LST to provide directions in mitigating climatic impacts and bolster sustainability initiatives locally based on available empirical evidence. The integration of these biophysical factors into analysis helps gain a comprehensive understanding of how urbanization impacts surface temperature and potentially affects the overall natural environment. Furthermore, this knowledge may support long-term benefits for resource management while considering urban planning strategies within a natural environment [14].

Whenever biophysical components come into consideration as environmental components, it indicates soil moisture, vegetation coverage, water bodies, and greenery, i.e., those influencing the LST [8,9]. Also, the relationship between LST and biophysical components is inherently linked to the spatial distribution of species and vegetation, which plays a critical role in regulating surface temperatures [15–17]. A significant challenge in ecological transformations lies in the conversion of vegetation and open spaces into developed surfaces, exacerbating environmental concerns and necessitating careful land use planning policies and conservation strategies [18,19]. Hence, it is crucial to establish a thorough understanding of the correlations between ecological changes in urban environments and their impact on LST changes for effective environmental management [18,19]. This study seeks to elucidate the intricate interplay between biophysical factors and LST, providing insights into their impacts on urban thermal dynamics [20].

In the context of South Asian cities, the expansion of urban areas and alterations to surface characteristics may significantly affect LST, resulting in modifications to the thermal dynamics of the environment [1]. Several research papers have supported the shifting of the LST regime once urbanization processes happen significantly in and around cities [21,22]. Moreover, scholars have emphasized that LST is a critical parameter for assessing the ecological equilibrium and fostering environmental sustainability [23–26]. Within the realm of ecological and environmental monitoring schemas, important indicators such as NDBI,

NDWI, and NDBAI demonstrate strong correlations with LST. It is worthwhile to note that the relationship between LST and several sensitive environmental indicators in cities across the south are important to assess in understanding the vulnerability of ecosystems and landscapes.

This study was designed to investigate the interplay between LST and environmental dynamics in Dhaka metropolitan area, along with the adjacent regions such as Gazipur and Narayangonj. Recently, these areas have been experiencing rapid urbanization and environmental transformation to accommodate the growing number of populations intensifying ecological challenges. Rapid urban growth in these regions has led to the loss of green infrastructure and permeable surfaces, increasing surface temperatures and making environmental management a pressing concern [27–29]. As a result, findings from this study may provide valuable insights to explore how biophysical dynamics interact with LST and how sustainable infrastructure can mitigate UHI effects in a fast-growing metropolitan region in the global south.

This research employs spatial science methods upon integrating Google Earth Engine (GEE) and Geographical Information System (GIS) platforms to process and analyze long-term satellite data (1993–2023). Analysis reveals that indices associated with LULC and biophysical measures are directly impacting LST. By leveraging GEE and GIS spatial analysis tools, this research unravels the importance of biophysical dynamics to combat extreme LST changes by providing insights into how urban expansion and ecological shifts influence surface temperature regimes. Afterward, this research paper investigated the complex relationship between LST and UHI upon considering available indices computed using tools in spatial science. Consequently, the study attempted to tackle two significant issues based on quantifiable information in Bangladeshi cities, considering UHI and biophysical degradation that directly impact public health and sustainable urban development policies. The findings highlight the importance of preserving and enhancing urban vegetation and water bodies to mitigate the negative thermal impacts happening due to rapid urbanization [30].

The major goal of this research article was to investigate how rapid urbanization influences the UHI dynamics by damaging natural biophysical components in South Asian megalopolises, particularly for Dhaka and surrounding areas. Specifically, this research examines how biophysical factors, such as vegetation, water bodies, and soil moisture contribute to thermal regulation and urban resilience. Moreover, the purpose of this research was to assess the efficacy of sustainable infrastructure and ecologically conscious urban design techniques in reducing the negative effects of urbanization on natural biophysical components, including water bodies, and reducing LST. Also, it aimed to uncover the interrelationships among important variables responsible for UHI while affecting natural environments.

Furthermore, the novelty of this research lies in demonstrating the importance of biophysical factors in addition to understanding the UHI impacts in urban areas. Prior studies have mostly illustrated the diverse applications of geophysical factors in environmental assessments, encompassing everything from air quality monitoring to comprehending temperature anomalies [28,31]. However, the intellectual significance of this study lies in its contribution to the ongoing discourse surrounding urban environments by emphasizing the complex role of biophysical components and uncovering their multifaceted implications across disciplines. Consequently, the study offers practical guidance for policymakers to develop sustainable urban planning strategies that can address the challenges posed by climate change.

2. Materials and Methods

2.1. Study Area

Dhaka, Bangladesh's capital and its largest city, is a burgeoning metropolis located at 23°42′ N, 90°22′ E (Figure 1), and stressed with demographic pressures and rapid

urbanization [32]. The city's growth is characterized by industrial and economic activities that have led to a rise in surface temperatures, eventually catering to the UHI effect [33].

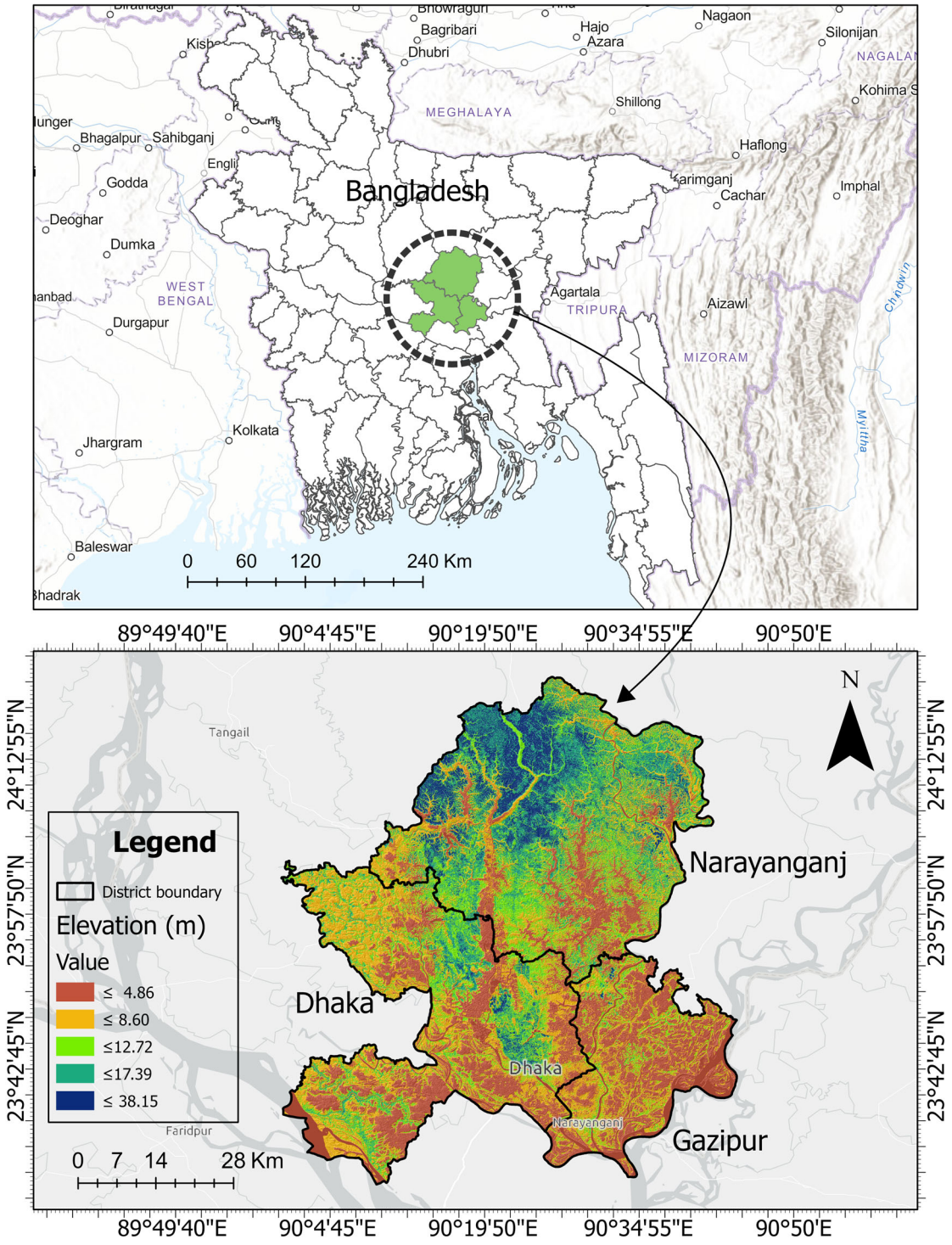

Figure 1. Map demonstrating the study area.

This urban growth and expansion are not confined to Dhaka only, but the wave extends to Gazipur and Narayanganj, eventually contributing to LST changes. Gazipur has seen a boom in commercial activities, particularly in the textile and garment industries, contributing to regional economic development [34]. Narayanganj, on the other hand, is relatively smaller in area (i.e., 113.98 km^2) and has experienced significant urban chal-

lenges [35]. The influx of people seeking employment opportunities in these industrial hubs has led to resource constraints, highlighting the need for sustainable urban planning [36].

In addition, Gazipur, Narayanganj, and other urban regions are rapidly evolving into major industrial hubs in Bangladesh [27,37]. Gazipur and Narayanganj, in particular, have emerged as vital nodes for industrial development, hosting a wide range of manufacturing-, textile-, and export-oriented industries. The rapid urbanization and industrialization in these areas have led to a significant expansion of built-up area, putting pressure on the surrounding environment. Moreover, these districts are highly sensitive to environmental changes, including issues such as ecological degradation, river pollution, and land subsidence [28]. Considering these factors, this study focused on these districts not only for understanding their economic and industrial significance, but also assessing their ecological impacts and the broader implications of urban growth in the natural environment [28,29].

2.2. Datasets

Satellite images, including Landsat 5 TM for 1993, 1999, Landsat 7 ETM+ for 2005, 2011, and Landsat 8 OLI and TIRS for 2017, and 2023, were collected for LULC classification and generating multiple indices. The obtained datasets had 30 m spatial resolution with less than 1% cloud coverage to ensure data quality. Indeed, high-quality data having minimal cloud interference ensured precise land cover classification and enhanced the accuracy assessment protocols. GEE facilitated the selection of the training data for classification and model validation purposes. Further details regarding data acquisition processes are summarized (Table 1).

Table 1. Description of the datasets used in this study.

Period (Year)	Timeframe (Month)	Dataset	Bands	Sensor	Spatial Resolution
1993	11 April	Metadata from Landsat 5, Level two,	1 to 7	Landsat 5 TM	30
1999	9 April				
2005	18 May	Metadata from Landsat 5, Level two,	1 to 7	Landsat 5 TM	30
2011	12 April				
2017	5 May	Metadata from Landsat 8, Level Two,	2 to 7	Landsat 8 OLI	30
2023	13 May				

Additionally, the years 1993, 1999, 2005, 2011, 2017, and 2023 were chosen to obtain information about land use change in the Dhaka, Narayanganj, and Gazipur districts. These years were aligned with key milestones of infrastructure development, industrialization, and population growth in the region [38,39]. For instance, the rapid urban expansion and growing industrial activities were reflected in the 1990s and 2000s [28,40]. The chosen years offered a comprehensive view of long-term urbanization trends, ensuring that both gradual changes and periods of accelerated land use transformation were adequately represented in the analysis.

2.3. Image Preprocessing and Classification

To avoid any seasonal and temporal variation among the imageries, all Landsat Annual imageries were gathered. The duration of the period was (April to May) for each year, and the average radiance was calculated for each pixel. Moreover, cloud coverage pixels were identified and considered only when less than 1% cloud-contaminated pixels were present. The imageries were further processed through cloud masking and saturation threshold, and filtered by boundary area.

Image classification stands as the cornerstone in detecting and quantifying LULC change through remote sensing methodologies. It involves grouping pixels from satellite imageries into similar data types, a task crucial for this research [41,42]. Four distinct LULC classes were considered in this study (see Table 2). Employing the Random Forest (RF) algorithm in the GEE cloud platform, a supervised machine learning image classification

technique was employed. Hyperparameter tuning was further applied to enhance accuracy, ensuring optimal parametric values. Training samples, meticulously gathered from field data and expert knowledge, spanned the years 1993, 1999, 2005, 2011, 2017, and 2023. On average, over 500 points were collected per land class, with 70% utilized for training and 30% for testing.

Table 2. Description of the land classes considered in this study.

Land Cover	Description
Vegetation	Natural and afforested dense forest, grass, or vegetated area
Barren land	Open land, field, playground, newly accreted land
Built-up	Business, factories, residential, transportation, streets, mixed downtown, and other developed area
Waterbody	River, canal, drainage channels, other active meteorological elements

2.4. Evaluation Metrics

The overall accuracy, user accuracy, and producer accuracy were chosen to assess classified data and crosscheck individual classes from the entire dataset. The Kappa coefficient statistics were adopted to evaluate the classified imageries and then compared with actual data obtained from the field. The ROC (receiver operating characteristic) and AUC (area under the curve) were selected to evaluate the model's ability to distinguish between classes at varying decision thresholds. These metrics were deemed relevant due to their widespread use in multi-class classification and their robustness in remote sensing applications [41].

The Kappa values reported for each district signified the reliability of the classification results by measuring the agreement between the classified images and ground truth data, and were eventually adjusted for chance agreement. In general, Kappa values range from -1 to 1, with higher values indicating stronger agreement [43]. According to widely accepted thresholds in the literature, Kappa values above 0.80 are considered excellent, values between 0.60 and 0.80 substantial, and values between 0.40 and 0.60 indicate moderate agreement [43,44]. In this context, higher Kappa values suggest a more reliable classification, while lower values indicate less consistent performance across districts.

To determine the correctness of the evaluation, the following equations were used (1)–(4) [45,46]:

$$\text{Overall precision} = \frac{\text{number of accurately categorized images is 100.}}{\text{Sum of all indicate images}} * 100 \quad (1)$$

$$\text{User precision} = \frac{(\text{total correct classified pixels in every class (diagonal)})}{\text{the sum of all source images in each class (the entire grid)}} * 100 \quad (2)$$

$$\text{Producer precision} = \frac{(\text{total correct classified pixels in every class (diagonal)})}{\text{Maximum number of referencing images in all groups (sum row)}} * 100 \quad (3)$$

$$\text{Kappa Coefficient (T)} = \frac{\text{Overall number of Sample} * \text{Corrected Sample} - \sum(\text{column.tot} * \text{row tot})}{(\text{The entire of Sample})^2 - \sum(\text{column.tot} * \text{row tot})} * 100 \quad (4)$$

User and producer accuracy offer a comprehensive evaluation by addressing different aspects of classification. The UA indicates how accurately a pixel is classified into a specific category truly belongs to that class from the user's perspective. In contrast, PA measures the classifier's ability to correctly identify the actual pixels in each class, preventing underrepresentation of true land cover [47,48]. The F1-score, which combines precision and recall is particularly helpful for handling imbalanced classes. Additionally, overall accuracy, Kappa coefficient, and AUC provide deeper insights into model performance and class differentiation, ensuring a robust assessment of accuracy.

The ROC curve, although tricky to read, is critical [49]. Equations (5) and (6) provide the two types of rate values (TPR and FPR) over the classification criteria. It carefully shows the relationship across these levels using the two metrics.

$$\text{TPR} = \frac{\text{True Positive}}{\text{True Positive} + \text{False Negative}} \tag{5}$$

$$\text{FPR} = \frac{\text{False Positive}}{\text{Fasle Positive} + \text{True Negative}} \tag{6}$$

$$\text{AUC} = \int_0^1 TPR\text{d}(\text{FPR}) \tag{7}$$

The ROC curve balances TPR and FPR for classification models to maximize efficacy in the leftmost position. Equation (7) quantifies the accuracy of models as AUC, with greater AUCs suggesting superior categorization. Thus, the ROC curve summarizes accuracy in changing evaluation methods [50].

2.5. Extraction of LST

The estimation of seasonal LST involved the utilization of DN from the thermal bands of the imageries, specifically Band 6 for Landsat 5 TM, and Bands 10 and 11 for Landsat 8 OLI. Initially, the application of Equations (9) and (10) was executed, leveraging the spectral radiance (λ) pertinent to the bands of Landsat 5 and Landsat 8 satellite image, consequently. Subsequently, employing the resultant values denoted as L, λ, the determination of LST in degrees Celsius was achieved using Equation (14). This meticulous methodological approach enabled the accurate inference of LST from the DN acquired through the thermal bands of the respective datasets. Landsat satellites ensured accuracy and reliability in the estimation process [51].

$$L_\lambda(\text{LANDSAT 5 TM}) = Lmin + + \frac{L_{max} - L_{min}}{Qcal_{max} - Qcal_{min}} \times DN \tag{8}$$

$$L_\lambda(LANDSAT\ 8\ OLI) = ML \times DN + AL \tag{9}$$

$$LST = \frac{T}{1 + \left(\lambda \times \frac{T_B}{\rho} * \ln(\varepsilon)\right)} - 273.15 \tag{10}$$

AL (0.1) is additive and ML (0.0003342) nonlinear (altering ratio varied by spectrum). The imagery dataset file comprised Landsat TM, L_{max}, and L_{min}. Radiant discharges possess a 11.5 µm duration [51,52].

$$\rho = \frac{\text{h} \times \text{c}}{\sigma} = 1.438 \times 10 - 2\ \text{mk} \tag{11}$$

h is the value of, 6.626×10^{34}Js, c is the light velocity, σ is the constant value by Boltzmann $5.67 \times 10^{-8} Wm^2k^{-4} = 1.38 \times 10^{-23} JK^{-1}$ Equation (11); ε is actually the emissivity value of land surface, ranging between 0.97 and 0.99.

$$TB = \frac{K_2}{In\left(\frac{K_1}{K_\lambda} + 1\right)} \tag{12}$$

where TB is the brightness temperature of satellite, and K_1 and K_2 are the constant values for Landsat 5 (607.7 and 1260.6, respectively) and for Landsat 8 (774.9 and 321.07, respectively) [52].

2.6. Acquisition of Biophysical Variables

The study employed remote sensing techniques and statistical analyses to explore the relationship between urban expansion and environmental dynamics, specifically targeting

LULC changes and their effects on LST. To achieve this, Landsat satellite imageries were used to detect LULC changes, employing a Random Forest classification algorithm within the GEE platform. This method was well-suited for providing an accurate classification of urban, vegetation, and water bodies. LST was calculated using thermal bands from the same satellite imageries, while indices such as NDVI, NDBI, NDWI, MNDWI, NDBAI, BSI, SAVI, and MSI helped quantifying changes in vegetation, built-up areas, and water bodies, respectively. Correlation analysis and PCA were applied to assess the interaction between urban expansion and biopsychical indices such as NDVI, NDWI, NDBI, NDBSI, MNDWI, BSI, SAVI, and MSI. These methodologies were appropriately selected based on scientific literature to delineate the relationships between LST and urban built-up environment [53]. Detailed discussions on these indices are provided in subsequent sections (Table 3).

Table 3. Formulas used for assessing the biophysical indices in this study.

Index Name	Index Name and Equation	References
Normalized difference vegetation index	$\mathrm{NDVI} = \frac{\mathrm{NIR}-\mathrm{RED}}{\mathrm{NIR}+\mathrm{RED}}$	[54,55]
Normalized difference water index	$\mathrm{NDWI} = \frac{\mathrm{GREEN}-\mathrm{NIR}}{\mathrm{GREEN}+\mathrm{NIR}}$	[56]
Normalized difference built-up index	$\mathrm{NDBI} = \frac{\mathrm{SWIR}-\mathrm{NIR}}{\mathrm{SWIR}+\mathrm{NIR}}$	[57]
Normalized difference bare soil index	$\mathrm{NDBSI} = \frac{(\mathrm{RED}+\mathrm{SWIR})-(\mathrm{NIR}+\mathrm{BLUE})}{(\mathrm{RED}+\mathrm{SWIR})+(\mathrm{NIR}+\mathrm{BLUE})}$	[58]
Modified normalized difference water index	$\mathrm{MNDWI} = \frac{\mathrm{Green}-\mathrm{MIR}}{\mathrm{Green}+\mathrm{MIR}}$	[59]
Bare soil index	$\mathrm{BSI} = \frac{\mathrm{NIR}-\mathrm{RED}}{\mathrm{NIR}+\mathrm{RED}}$	[60]
Soil-adjusted vegetation index	$\mathrm{SAVI} = \left(\frac{\mathrm{NIR}-\mathrm{RED}}{\mathrm{NIR}+\mathrm{RED}+\mathrm{L}}\right) * (1+L)$	[61]
Moisture stress index	$\mathrm{MSI} = \frac{\mathrm{NIR}-\mathrm{SWIR}}{\mathrm{NIR}+\mathrm{SWIR}}$	[62]

After normalizing the parameters utilized in this study, correlation analysis was performed to explore their relationships. The equations employed for parameter normalization in this research are as follows:

$$\mathrm{Positive} = \frac{\mathrm{A} - A_{min}}{A_{max} - A_{min}} \tag{13}$$

$$\mathrm{Negative} = \frac{A_{max} - \mathrm{A}}{A_{max} - A_{min}} \tag{14}$$

where A indicates the actual value, and A_{max} and A_{min} refer to the highest value and lowest value.

2.7. Statistical Analysis

In this analysis, we used both descriptive and inferential statistics to recognize how biophysical characteristics impact LST. Statistical tests were conducted to assess the significance of the variations across different years. An ANOVA (analysis of variance) [63] was applied to determine if the observed differences in precision were statistically significant [63]. The results indicated whether there was a significant variation in precision over time. If the test showed a low *p*-value (typically less than 0.05), it was suggested that the differences in precision across years were statistically significant.

2.7.1. Correlation Matrix

The Pearson correlation coefficient (r) has emerged as a tool in unraveling the relationship between LST and various ecological indices. It is widely recognized that geophysical indices significantly shape LST, with spatial variations in urban thermal environments [64]. Denoted as "r", Pearson correlation serves as a measure of the extent to which these data

points deviate from the line of optimal approximation [65]. The correlation matrix among the biological variables and LST have been calculated along with the scatterplot.

2.7.2. Principal Component Analysis (PCA)

In this study, the PCA (illustrate Figure 2) tool evaluated spatial relationships between variables. We utilized PCA to investigate the elements that influenced seasonal temperature anomalies in the study area. This method is typically used to mitigate the discrepancies of the dataset [66].

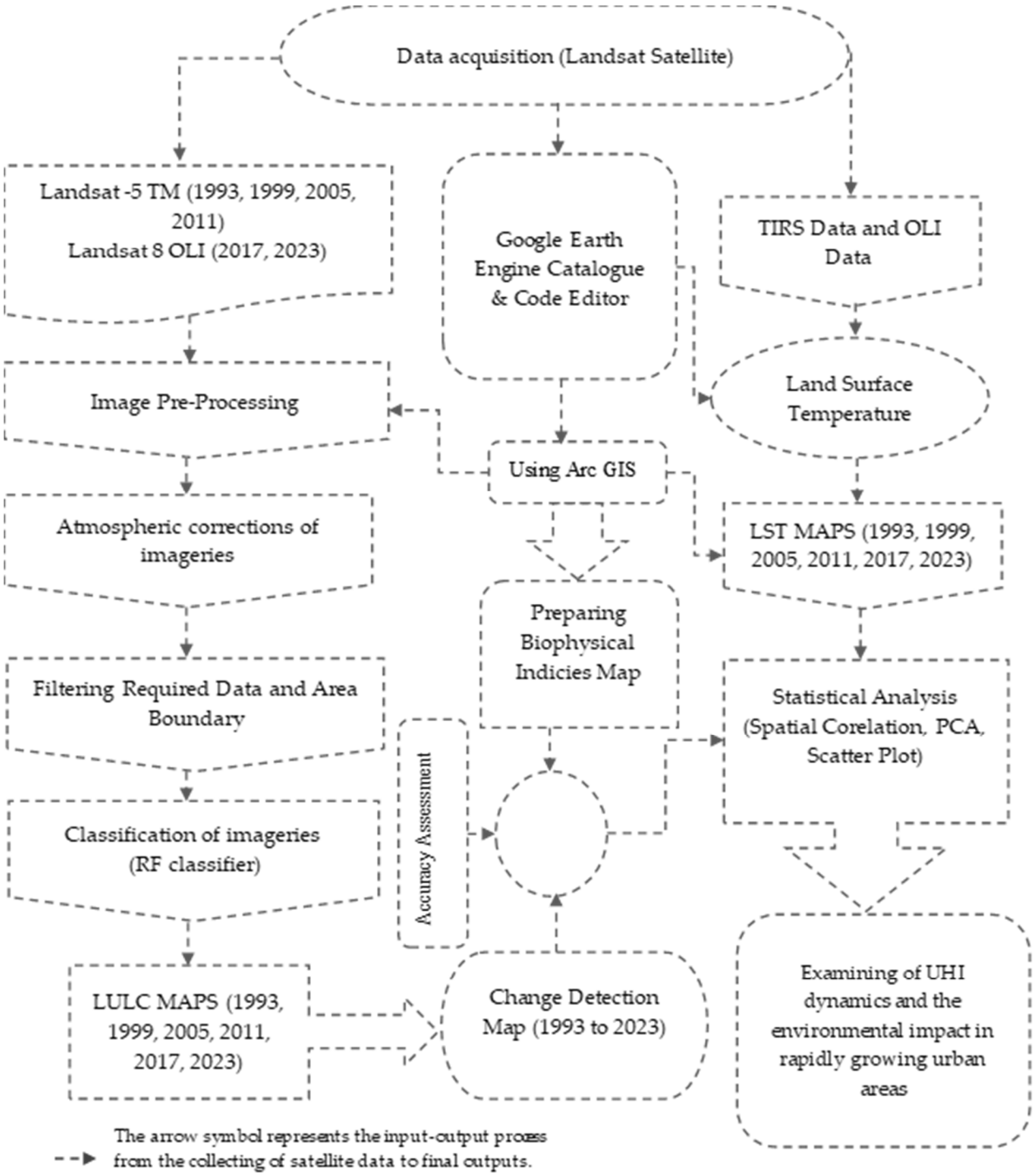

Figure 2. Schematic diagram of the methods adopted in the study.

3. Results

3.1. Accuracy Assessment

The evaluation included essential metrics in Table 4, for precision assessment, encompassing the years 1993, 1999, 2005, 2011, 2017, and 2023. Evaluations were conducted on several measures of precision, such as total precision, correctness for producers, consistency for users, and Kappa values. The total precision of the LULC result varied notably throughout the study period, ranging from 85.20% to 89.93% for Dhaka, 83.89% to 88.27% for Narayanganj, and 83.89% to 93.84% for Gazipur, respectively. Also, among the decades that were mentioned, the Kappa dependability varied between 0.852 and 0.912 for Dhaka, 0.859 and 0.962 for Narayanganj, and 0.862 and 0.912 for Gazipur. Around 1993–2023, the Kappa values spanned 0.882–0.897, 0.86–0.887, and 0.854–0.91.

Table 4. Evaluation of the classified images' accuracy.

		User Accuracy (%)				Manufacturer Precision (%)					
	Year	Built-Up	Waterbody	Barren Land	Vegetation	Built-Up	Waterbody	Barren Land	Vegetation	Total Precision	Kappa Statistics
Dhaka	1993	0.85	0.89	0.83	0.90	0.90	0.86	0.76	0.86	89.93%	0.893
	1999	0.85	0.89	0.76	0.93	0.85	0.86	0.76	0.94	86.49%	0.909
	2005	0.92	0.89	0.82	0.89	0.95	0.96	0.75	0.87	85.20%	0.901
	2011	0.85	0.89	0.90	0.89	0.96	0.87	0.81	0.91	88.98%	0.940
	2017	0.88	0.89	0.77	0.84	0.97	0.93	0.68	0.84	86.09%	0.876
	2023	0.94	0.89	0.83	0.74	0.93	0.91	0.68	0.84	83.09%	0.846
Narayanganj	1993	0.88	0.88	0.89	0.96	0.88	0.89	0.98	0.95	86.79%	0.883
	1999	0.89	0.88	0.86	0.81	0.90	0.93	0.96	0.93	86.04%	0.863
	2005	0.88	0.88	0.84	0.90	0.94	0.86	0.91	0.90	85.74%	0.872
	2011	0.87	0.87	0.84	0.88	0.92	0.95	0.86	0.91	88.27%	0.923
	2017	0.88	0.86	0.87	0.85	0.93	0.84	0.95	0.83	83.89%	0.882
	2023	0.91	0.87	0.73	0.80	0.93	0.88	0.73	0.76	85.63%	0.859
Gazipur	1993	0.73	0.89	0.81	0.88	0.87	0.88	0.81	0.98	83.89%	0.878
	1999	0.81	0.88	0.84	0.89	0.81	0.89	0.84	0.85	85.01%	0.887
	2005	0.90	0.89	0.82	0.93	0.88	0.88	0.89	0.95	86.69%	0.887
	2011	0.90	0.87	0.84	0.89	0.96	0.89	0.78	0.85	93.84%	0.869
	2017	0.85	0.87	0.84	0.82	0.92	0.87	0.75	0.91	88.56%	0.878
	2023	0.89	0.87	0.68	0.78	0.93	0.88	0.84	0.87	87.05%	0.922

Furthermore, from 1993 to 2023, the "Interactive" group shone out with a F1score that spans 0.899–0.851, recall metrics encompassing 0.869–0.897, and accuracy scores varying from 0.952 to 0.919 (refer to Appendix A, Table A1).

3.2. LULC Dynamics

The selection of specific time intervals, 6 years apart from 1993 to 2023 was made to reflect the gradual nature of LULC changes (Table 5 and Figure 3) which typically occurred over extended periods rather than in rapid succession. Urban expansion and environmental dynamics often unfolded slowly due to factors like urban planning, regulatory processes, and the time required for natural ecosystems to respond to anthropogenic influences. Thus, a longer interval allowed for a more accurate representation of substantial shifts in land use.

Table 5. Area (sq km.) and LULC change from 1993 to 2023.

District	Year LULC	1993	1999	2005	2011	2017	2022	1993–1999	1999–2005	2005–2011	2011–2017	2017–2023
Dhaka	Built-up	94.95	208.12	240.79	221.62	275.09	434.08	113.17	32.66	−19.17	53.47	158.99
	Water body	566.9	657.1	473.82	465.46	634.95	427.73	90.2	−183.27	−8.37	169.5	−207.22
	Barren land	258.74	86.31	97.31	97.46	46.97	27.06	−172.42	11	0.16	−50.48	−19.91
	Vegetation	537.85	506.89	646.5	673.88	501.4	569.55	−30.95	139.61	27.38	−172.48	68.14

Table 5. *Cont.*

District	Year LULC	1993	1999	2005	2011	2017	2022	1993–1999	1999–2005	2005–2011	2011–2017	2017–2023
Gazipur	Built-up	51.81	90.39	85.05	131.38	122.56	242.84	−152.45	−5.34	46.32	−8.81	120.28
	Water body	341.32	399.92	370.23	415.1	358.66	380.53	19.39	−29.69	44.87	−56.45	21.88
	Barren land	275.62	217.18	220.49	238.47	184.22	46.85	170.33	3.33	17.98	−54.26	−137.37
	Vegetation	1082.54	1043.8	1075.51	966.33	1085.85	1081.08	−37.27	31.7	−109.18	119.52	−4.78
Narayanganj	Built-up	78.38	93.43	214.35	216.74	215.83	243.53	15.05	120.93	2.4	−0.92	27.7
	Water body	178.04	156.74	174.81	161.96	119.44	106.13	−21.29	18.07	−12.85	−42.53	−13.3
	Barren land	192.36	161.67	140.81	124.75	127.92	52	−30.7	−20.86	−16.06	3.19	−75.93
	Vegetation	231.55	268.5	150.37	181.38	217.15	278.67	36.95	−118.14	31.03	35.76	61.52

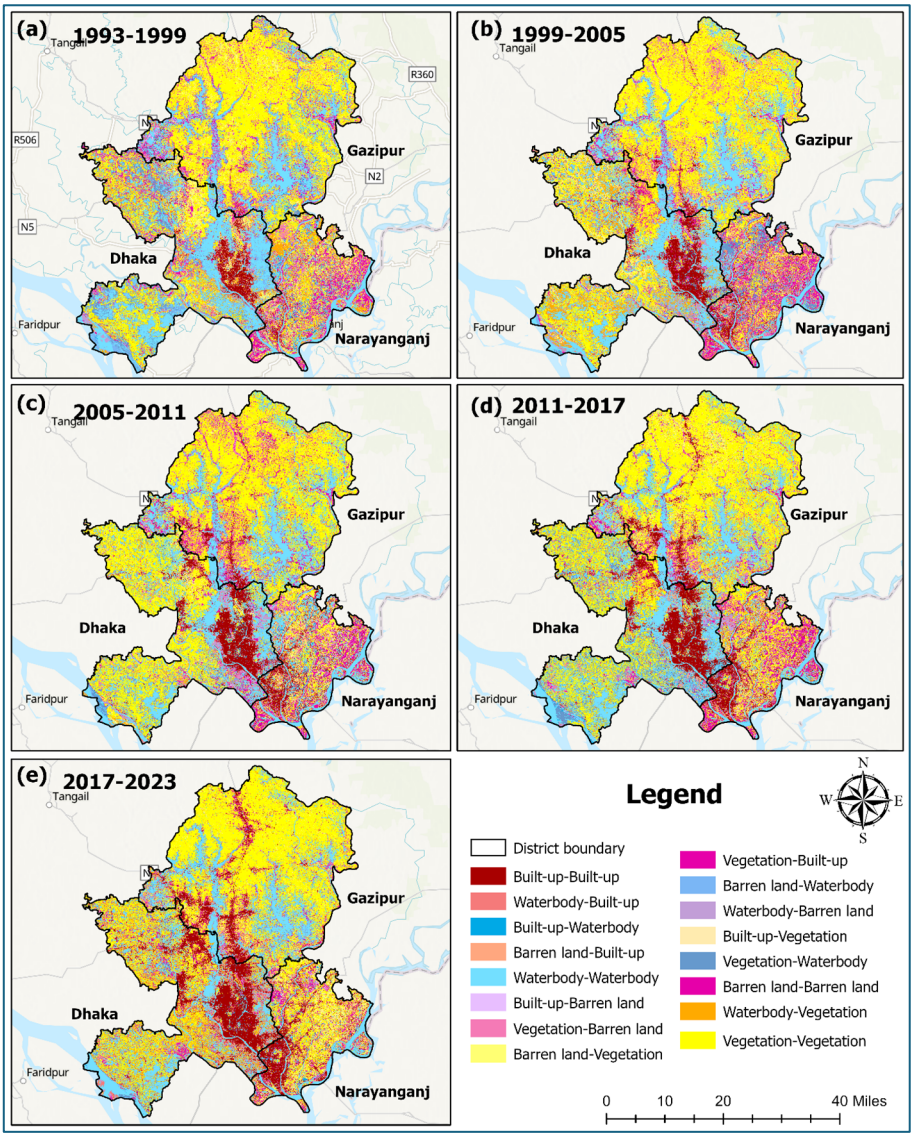

Figure 3. LUCCC in the Dhaka, Narayanganj, and Gazipur districts: (**a**) 1993–1999, (**b**) 1999–2005, (**c**) 2005–2011, (**d**) 2011–2017, and (**e**) 2017–2023.

While more frequent temporal resolutions could potentially offer insights into short-term fluctuations, they might not capture the broader, more significant trends that defined

LULC changes. Short intervals might lead to an oversimplification of complex processes, making it challenging to discern meaningful patterns in the data. The chosen intervals offered a balance, emphasizing the importance of long-term trends in urban expansion, while acknowledging that LULC transformations require time to manifest fully.

Dhaka's urbanization led to a substantial decrease in water bodies and barren land, primarily due to the influx of migration. This rapid urbanization led to a 57% decline in water bodies and a 91% reduction in barren land. The alteration of Dhaka's LULC highlighted the region's dynamism and adaptability, but also underscored the need for balance between development and ecological preservation.

The Gazipur district experienced significant urban expansion (Figures 4 and 5; Table 5) from 1993 to 2023, with an 83% increase in built-up area. This growth was driven by urban population and demands for infrastructural needs. Despite this, water bodies increased by 8%, indicating expanding city boundaries in the nearby hinterland and protecting their natural resources. The city's industrial status attracted migrants, further exacerbating the urbanization process. However, this rapid urbanization trajectory had consequences, as evident by the significant 30% reduction in vegetation cover during the same period. Failure to protect the green spaces not only disrupted the difficult ecological equilibrium, but also brought adverse implications for biodiversity and triggered the LST across urban and rural landscapes. The evolution of the Gazipur district displayed the intricate interplay between urbanization, industrialization, and environmental sustainability. As the region continued to chart its developmental course, striking balance between urban expansion and ecological preservation remained imperative to ensure the long-term resilience.

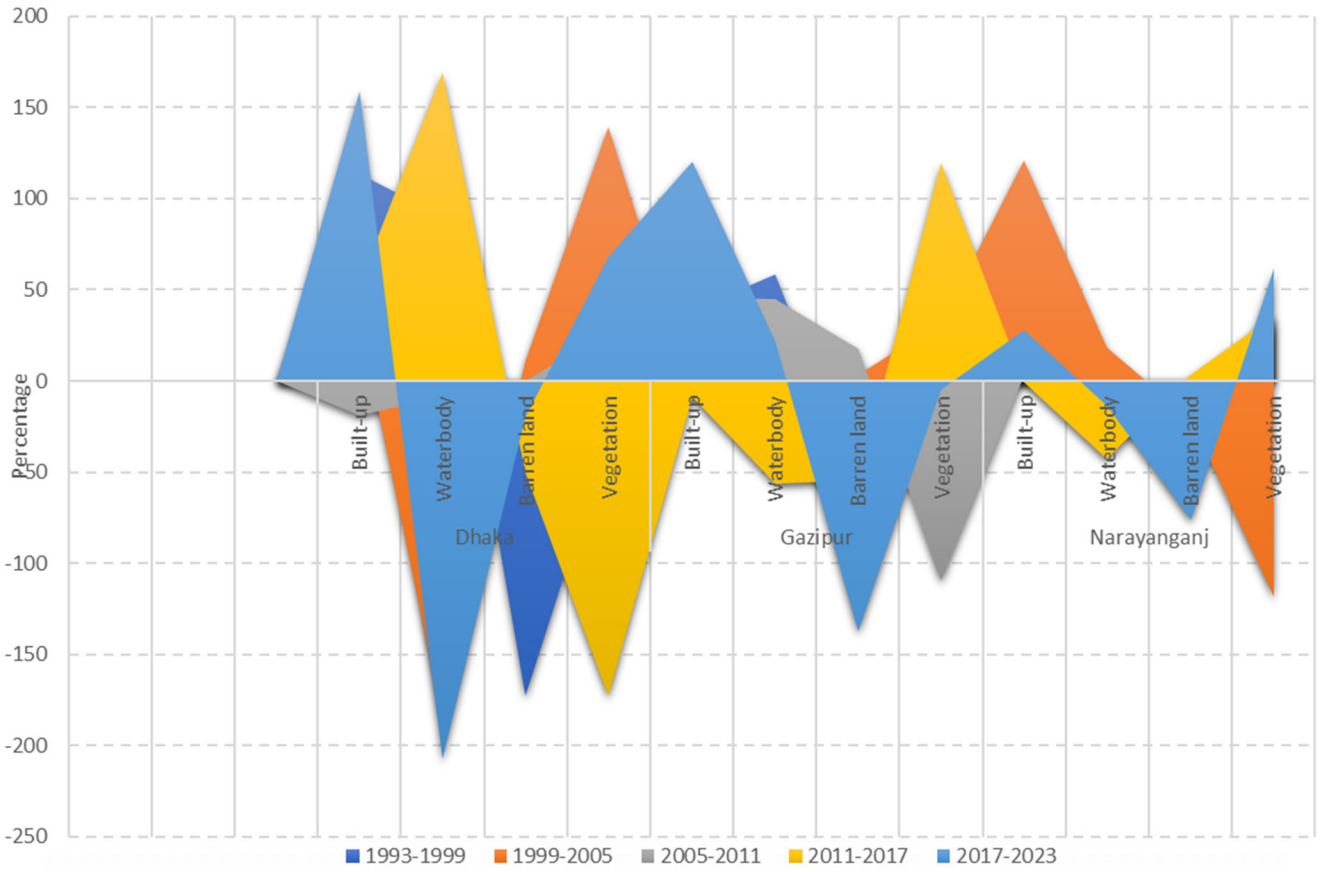

Figure 4. Representing the LUCCC dynamics in Dhaka, Narayanganj, and Gazipur.

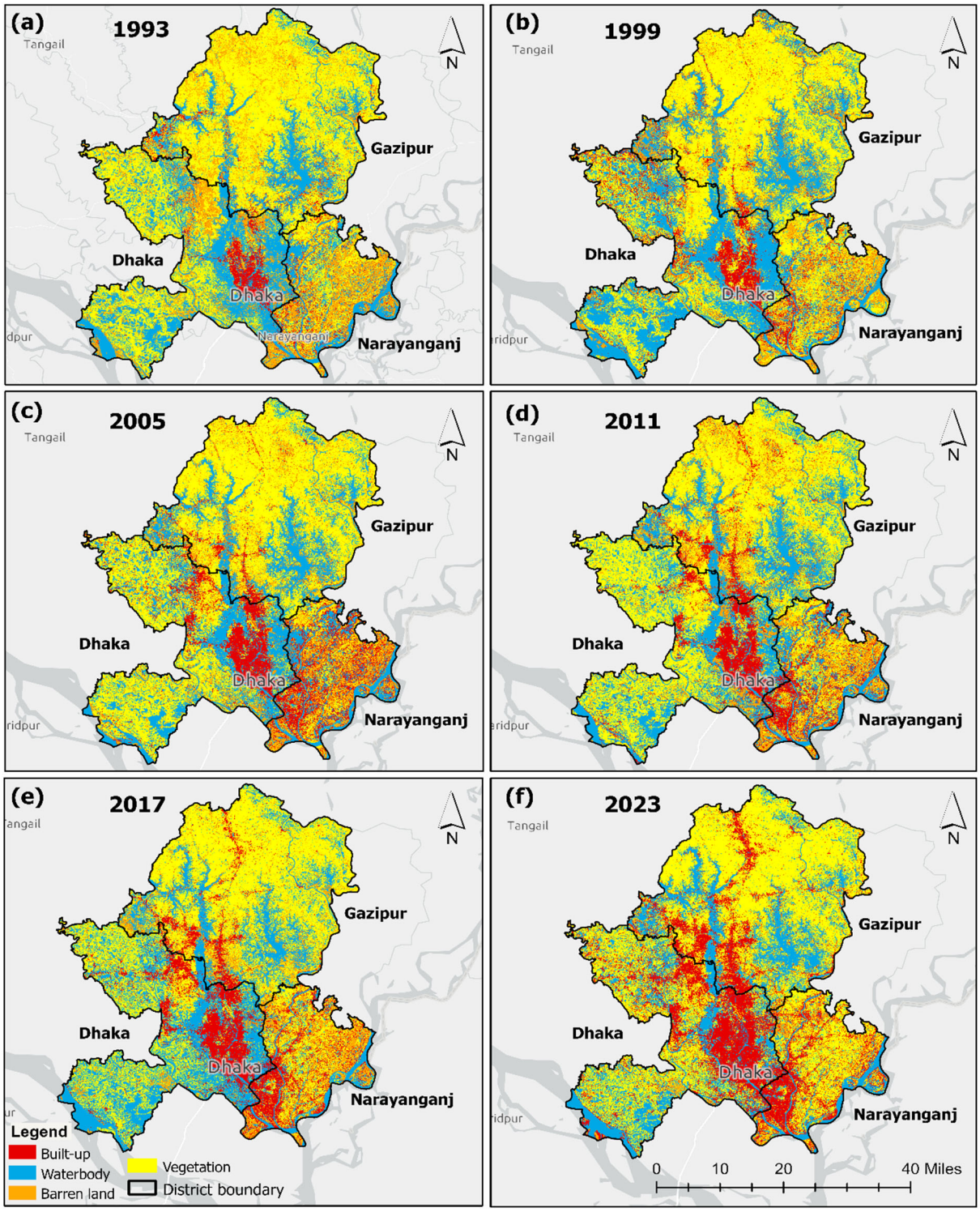

Figure 5. Land use classes in the Dhaka, Gazipur, and Narayanganj districts: (**a**) 1993, (**b**) 1999, (**c**) 2005, (**d**) 2011, (**e**) 2017, and (**f**) 2023.

The findings of the study show a staggering surge of over 199% in Narayanganj's total built-up area. Concurrently, the urban landscape of Narayanganj witnesses a huge decline of water bodies (i.e., around 43%). Moreover, there is a trend of decreasing vegetated surfaces across Narayanganj, which is around 23%. Gazipur and Narayanganj stand as a fundamental industrial hub that trigger the rapid urbanization. This urban transformation has facilitated the increase of vibrant commercial zones. Shifting LULC dynamics

were observed in the Dhaka, Gazipur, and Narayangonj districts, and underscored rapid urbanization, characterized by notable expansions in built-up areas.

One of the key differences observed was the rate of urban expansion. We recorded a significant urban expansion of 339.13 km^2 in the last 30 years, with an average annual growth rate of 3.5%. This rate of change was notably higher than what was observed in many developed regions, where urban growth tends to be more regulated and gradual. This rapid urbanization in South Asian cities led to a more pronounced UHI effect, highlighting the critical need for localized and adaptable LULC classification strategies.

The findings from Dhaka, Narayanganj, and Gazipur can be generalized to other rapidly urbanizing regions facing similar environmental challenges. Many developing countries experience LULC changes due to urban expansion, impacting local climates and increasing LST. Like these districts, other areas may confront issues such as deforestation, vegetation loss, and rising built-up zones, contributing to the UHI effect. This study offered a framework for analyzing LULC changes and their climatic impacts (i.e., LST in particular) in regions with comparable socio-economic conditions. By utilizing satellite imagery and remote sensing techniques, similar evaluations can be conducted elsewhere to explore the relationship between urban growth and environmental shifts.

However, generalizing these results to other regions may pose challenges due to varying urbanization patterns, socio-economic contexts, regulatory measures, and environmental factors. The methodology, reliant on Landsat data and summer month images, may not be suitable for other regions with a different context. Additionally, limitations in spatial resolution and regional specificity of data requirements may not capture local urban dynamics. Broader application may require comparative studies across diverse regions to validate the model.

3.3. Spatial Distribution Pattern of LST

Comparing different years using remote sensing imageries can still be appropriate despite temperature anomalies as the analysis accounts for these variations. By selecting imageries from the same season across different years, it helps control data skewness. While inter-annual fluctuations in temperature exist, the comparison of LST between years provides valuable insights into the long-term effects of urbanization and land use changes. Throughout 1993 and 1999, during a period of tremendous urban growth, 39.21% of the urban area's water body transformed to NDBI, and the city's regions showed maximum temperature at 31.087 °C (Figures 6 and 7).

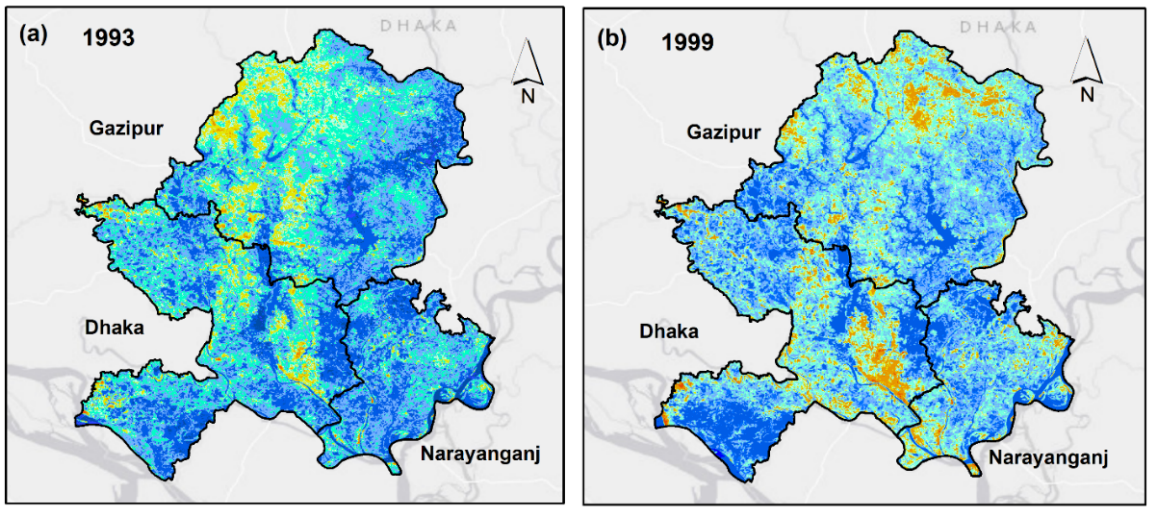

Figure 6. *Cont.*

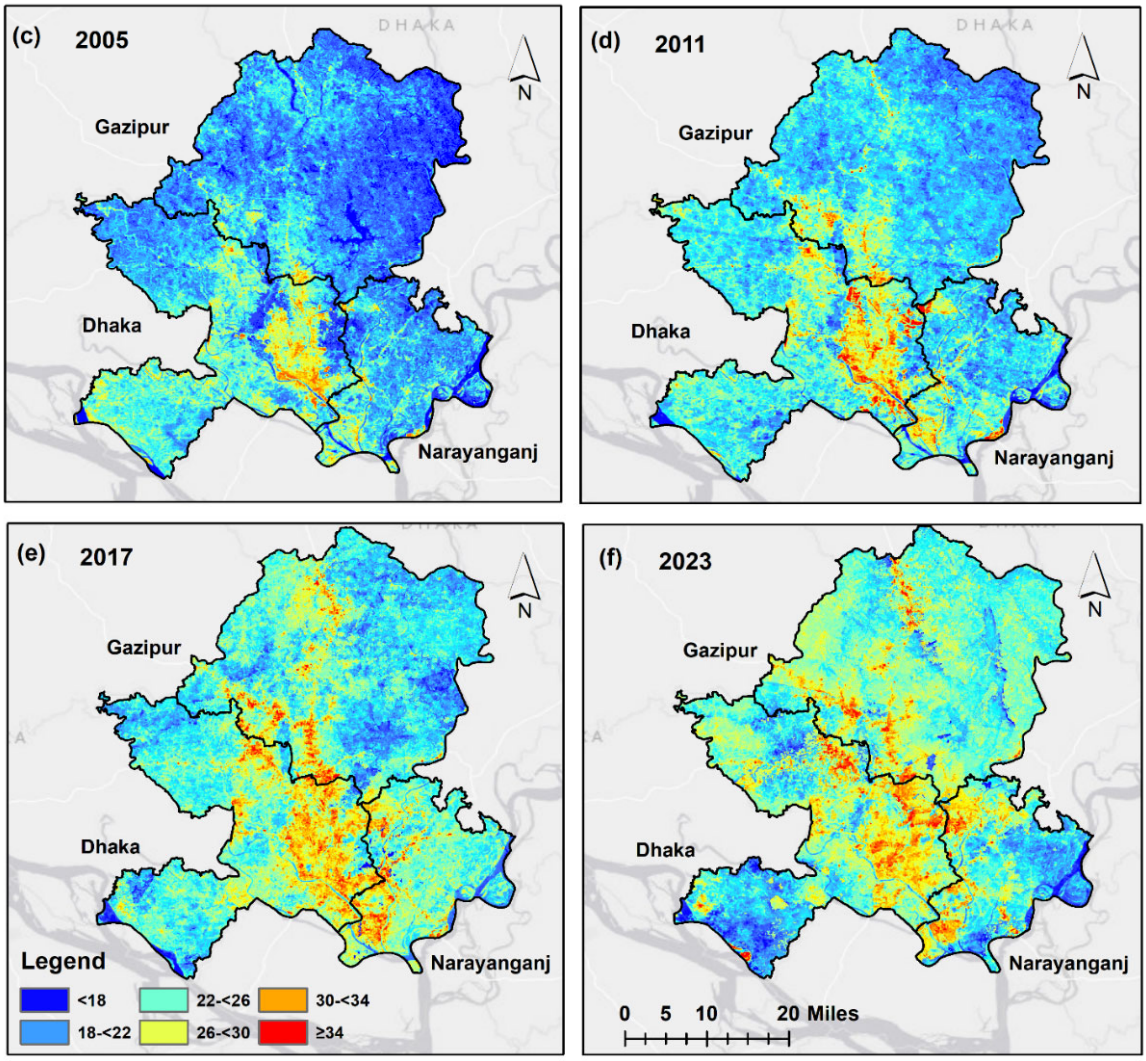

Figure 6. Spatial distribution of LST in the Dhaka, Narayanganj, and Gazipur districts: (**a**) 1993, (**b**) 1999, (**c**) 2005, (**d**) 2011, (**e**) 2017, and (**f**) 2023.

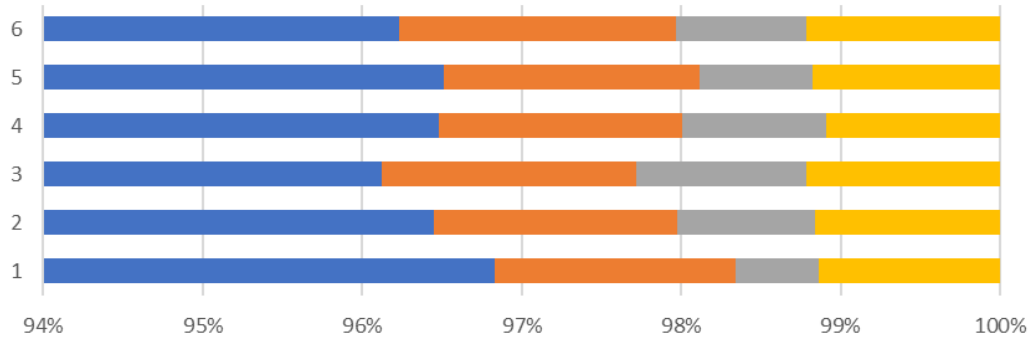

	1	2	3	4	5	6
Year	1993	1999	2005	2011	2017	2023
Maximum(°C)	31.087	31.6335	33.2229	31.7844	33.5067	36.5016
Minimum(°C)	10.8346	17.8783	22.2824	18.7642	14.8781	17.2098
Mean (°C)	23.34	24.02	25.31	22.73	24.55	25.58

Figure 7. Overall LST distribution (1993 to 2023).

Lowest temperature point of 19.92 °C and a transition of 10.17% from bare SVI to NDVI occurred between 1999 and 2005. This suggests that farming and ecological progress were slower at that time. On the other hand, the fastest rate of change occurred between 2017 and 2023, when the highest temperature was 36.52 °C. This pointed to a change in land use, either toward larger-scale expansion or toward the existence of empty space. The Gazipur and Narayanganj districts demonstrate the most notable change in LST from 2011 to 2017, which is approximately 33.51 °C. Also, the Narayanganj district shows the highest rate of temperature increase from 2017 to 2023, which significantly has risen to 31.44 °C. In 2017–2023, the Gazipur district has demonstrated upward trajectories and risen to 31.38 °C by 2023. Interestingly, this study ruminates that industrialization has been on the rise, particularly in the past decade. The increase in LST in urban environments appears to be caused by several causes, namely uncontrolled growth in urban areas, climate change, and the disappearance of geophysical indicators and surface water sources in the study area [67].

3.4. Pattern of the Biophysical Indices in Dhaka, Gazipur, and Narayangonj

This study addressed the potentials of confounding variables that may influence the relationships between LST and various biophysical parameters by employing Spearman's correlation method. This approach goes beyond mere numerical values, allowing for a deeper exploration of the complex interactions between LST dynamics and ecological parameters. By analyzing the coefficients of different independent variables, such as NDBI, NDBAI, BSI, SAVI, NDVI, MSI, NDWI, and MNDWI, this study carefully examined their individual and combined effects on LST, thus reducing the impact of potential confounding variables.

Moreover, this study considers multiple environmental factors influencing LST, providing a more nuanced understanding of influential relationships. This multi-dimensional examination enabled the study to identify both positive and negative correlations, highlighting the intricate interplay among variables and mitigating the risk of drawing misleading conclusions due to confounding influences.

The Dhaka, Gazipur, and Narayangonj districts are evolving with a significant shift in NDBI, NDBSI, MNDWI, SAVI, and MSI values. Detailed information is summarized above (Figures 8–10 and Table 6). The fluctuations in NDBI and NDBSI across the Dhaka district offers insightful variations observed over the study period. Notably, the maximal value of NDBI displays a gradual decline.

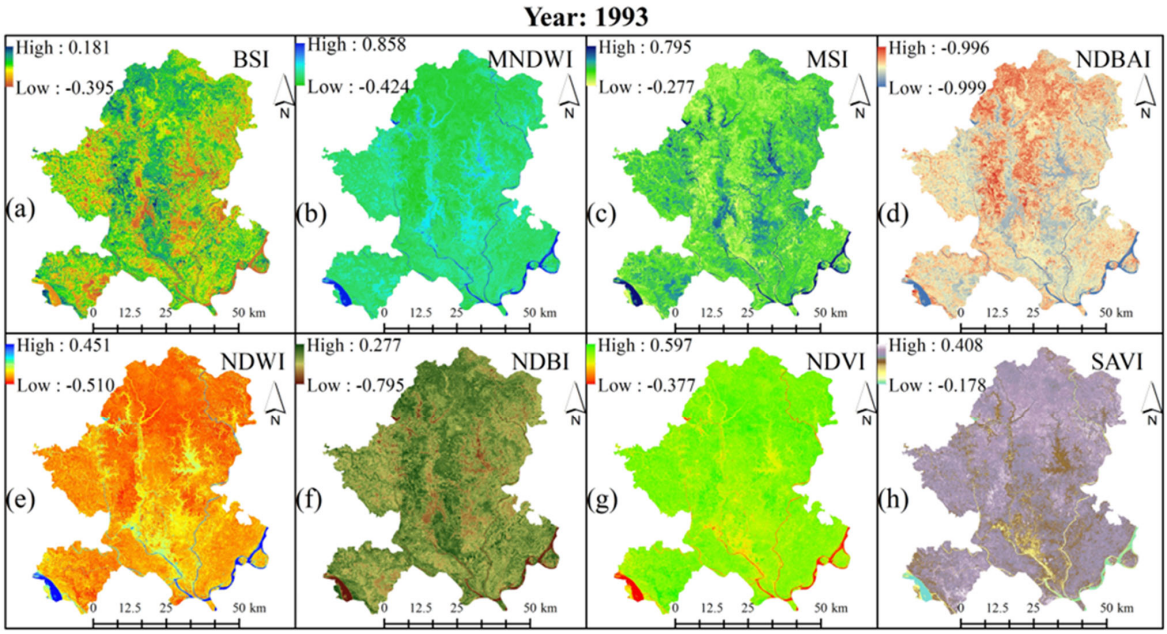

Figure 8. *Cont.*

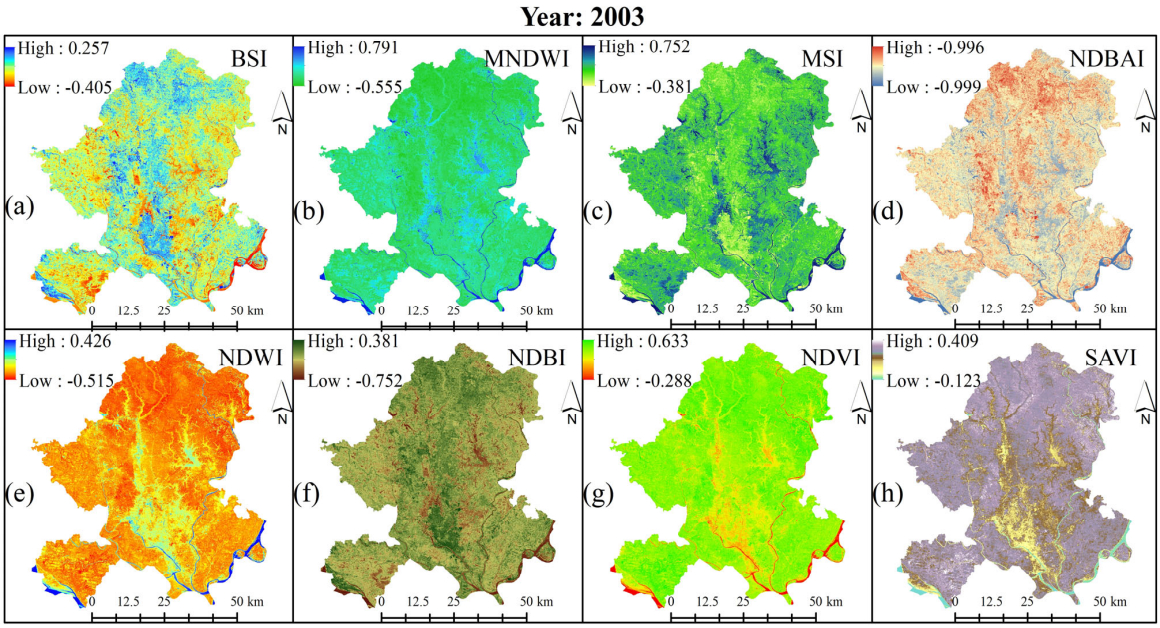

Figure 8. Spatial distribution of biophysical indices in the Dhaka, Gazipur, and Narayangonj districts in 1993 and 2003, (**a**) BSI, (**b**) MNDWI, (**c**) MSI, (**d**) NDBAI, (**e**) NDWI, (**f**) NDBI, (**g**) NDVI, and (**h**) SAVI.

Conversely, both NDBI and NDBSI decline to −0.773, while MNDWI, SAVI, and MSI also hit their lowest points at −0.710. Particularly, SAVI and MSI surge to their highest points at 0.726 and 0.552, respectively, shedding light on the intricate dynamics of vegetative health and surface moisture content. These observations underscore the urgency for a comprehensive policy framework aligned with these findings.

In Dhaka (Figure 8), the lowest values of NDVI, NDWI, and NDBAI were −0.335097, −0.795, and −1.000, respectively. The eastern, southern, and middle western parts of the city exhibited the lowest NDWI and bare impervious surfaces. Urgent integration of sustainable environmental strategies and green infrastructure into planning policies would require in this area. Noteworthy, fluctuations in NDWI were observed in the northern part, ranging from −0.795 to 0.438. Over twenty years, the maximum NDVI decreased from −0.335 to −0.833, and the minimum BSI declined from −0.207 to −0.471. Strategic planning and policy interventions would be critical for promoting sustainable urban development, aligning with environmental conservation goals.

Noteworthy (Figure 9), fluctuations in NDWI were observed in the northern part, ranging from −0.795 to 0.438. Over twenty years, the maximum NDVI decreased from −0.335 to −0.833, and the minimum BSI declined from −0.207 to −0.471. One of the main takeaways of this study was that predominant direction of change in NDWI and NDVI reduction within the Dhaka district, primarily attributed to the conversion of such areas into a commercial zone. Specifically, a wide area (i.e., 89.87 km^2) underwent conversion into the use of residential purposes, constituting 32.4% of the total changes of barren land were observed in the urban areas of Dhaka. This transformation was intricately linked to the central urban growth of Dhaka, leading to expansion of the city. Consequently, there arose a critical need to balance developmental demands with environmental conservation efforts considering these evolving trends. Furthermore, an anticipated consequence of the ecological alterations would be a notable shift in temperature dynamics, leading to an unexpectedly warmer and shorter winter season compared to historical patterns, as suggested by climate scientists [68].

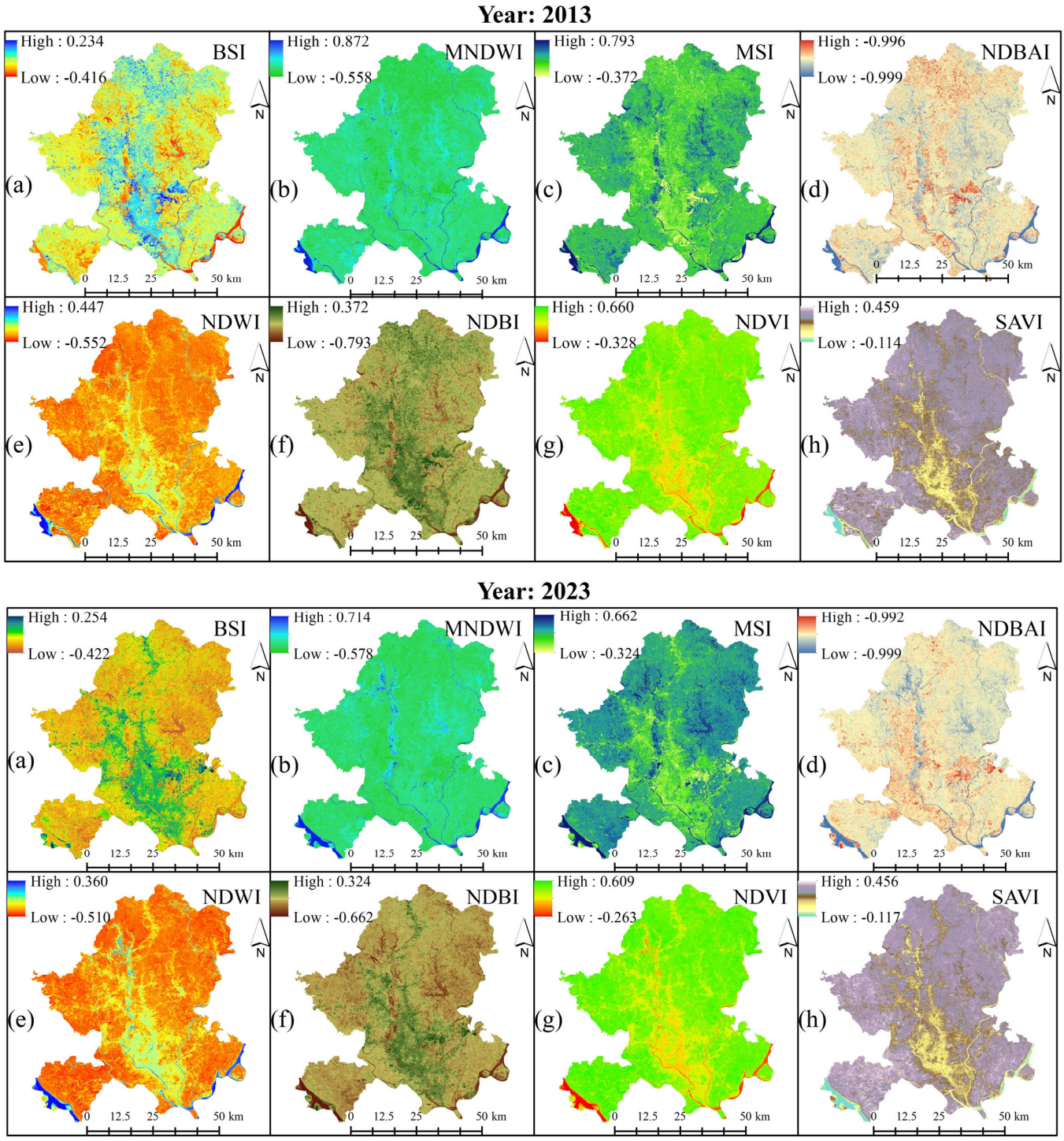

Figure 9. Biophysical features were distributed geographically in Gazipur, Narayanganj, and Dhaka districts from 2013–2023, (**a**) BSI, (**b**) MNDWI, (**c**) MSI, (**d**) NDBAI, (**e**) NDWI, (**f**) NDBI, (**g**) NDVI, and (**h**) SAVI.

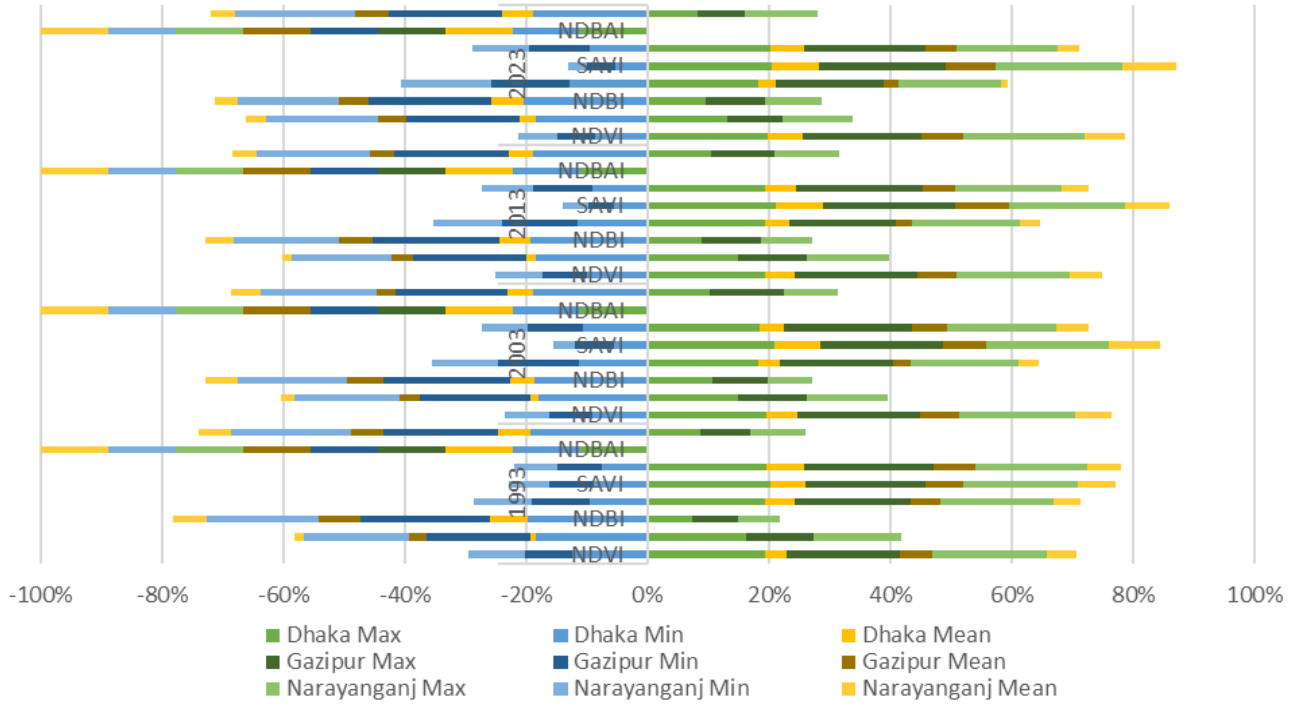

Figure 10. Descriptive statistics of the biophysical indices considered in this study.

Table 6. Descriptive statistics of the spatial indices considered in this study.

Year	District	Dhaka			Gazipur			Narayanganj		
	Biophysical Indices	**Max.**	**Min.**	**Mean**	**Max.**	**Min.**	**Mean**	**Max.**	**Min.**	**Mean**
1993	NDVI	0.597	−0.377	0.109	0.574	−0.241	0.166	0.578	−0.285	0.146
	NDWI	0.451	−0.510	−0.029	0.315	−0.475	−0.079	0.397	−0.485	−0.044
	NDBI	0.276	−0.733	−0.228	0.277	−0.795	−0.259	0.261	−0.683	−0.210
	MNDWI	0.858	−0.418	0.220	0.847	−0.422	0.212	0.830	−0.424	0.203
	SAVI	0.408	−0.178	0.115	0.396	−0.146	0.124	0.380	−0.134	0.122
	MSI	0.732	−0.276	0.228	0.795	−0.277	0.259	0.683	−0.261	0.210
	NDBAI	−0.99	−0.999	−0.998	−0.997	−0.999	−0.998	−0.996	−0.999	−0.998
	BSI	0.173	−0.383	−0.105	0.163	−0.377	−0.107	0.181	−0.395	−0.107
2003	NDVI	0.617	−0.288	0.164	0.633	−0.224	0.204	0.604	−0.231	0.186
	NDWI	0.426	−0.507	−0.040	0.323	−0.515	−0.095	0.377	−0.498	−0.060
	NDBI	0.381	−0.665	−0.141	0.328	−0.752	−0.212	0.266	−0.646	−0.189
	MNDWI	0.775	−0.480	0.147	0.791	−0.555	0.118	0.751	−0.468	0.141
	SAVI	0.409	−0.109	0.149	0.397	−0.123	0.136	0.398	−0.073	0.162
	MSI	0.665	−0.381	0.141	0.752	−0.328	0.212	0.646	−0.266	0.189
	NDBAI	−0.997	−0.999	−0.998	−0.996	−0.999	−0.998	−0.997	−0.999	−0.998
	BSI	0.222	−0.403	−0.090	0.257	−0.393	−0.067	0.191	−0.405	−0.107

Table 6. *Cont.*

Year	District	Dhaka			Gazipur			Narayanganj		
	Biophysical Indices	**Max.**	**Min.**	**Mean**	**Max.**	**Min.**	**Mean**	**Max.**	**Min.**	**Mean**
2013	NDVI	0.638	−0.328	0.155	0.660	−0.234	0.212	0.611	−0.259	0.175
	NDWI	0.447	−0.545	−0.049	0.335	−0.552	−0.108	0.406	−0.492	−0.042
	NDBI	0.344	−0.735	−0.195	0.372	−0.793	−0.210	0.321	−0.663	−0.172
	MNDWI	0.872	−0.518	0.177	0.787	−0.558	0.114	0.802	−0.506	0.147
	SAVI	0.443	−0.114	0.164	0.459	−0.091	0.184	0.401	−0.086	0.157
	MSI	0.735	−0.344	0.195	0.793	−0.372	0.210	0.663	−0.321	0.171
	NDBAI	−0.997	−0.999	−0.998	−0.996	−0.999	−0.998	−0.997	−0.999	−0.998
	BSI	0.232	−0.415	−0.0917	0.234	−0.416	−0.091	0.233	−0.412	−0.089
2023	NDVI	0.605	−0.263	0.171	0.599	−0.187	0.205	0.609	−0.195	0.207
	NDWI	0.360	−0.505	−0.072	0.252	−0.510	−0.129	0.315	−0.504	−0.094
	NDBI	0.310	−0.662	−0.175	0.324	−0.654	−0.164	0.300	−0.541	−0.120
	MNDWI	0.714	−0.494	0.109	0.691	−0.508	0.091	0.658	−0.578	0.0399
	SAVI	0.449	−0.117	0.165	0.456	−0.098	0.179	0.455	−0.067	0.193
	MSI	0.662	−0.310	0.175	0.654	−0.324	0.164	0.541	−0.300	0.120
	NDBAI	−0.996	−0.999	−0.997	−0.996	−0.999	−0.997	−0.996	−0.999	−0.997
	BSI	0.176	−0.399	−0.111	0.165	−0.396	−0.115	0.256	−0.422	−0.083

3.5. The Effect of Geophysical Characteristics on LST

The findings of this study underscore the considerable impacts of biophysiological indices on LST, corroborating previous research [69]. The correlation matrix output (presented in (Figures 11 and 12**)** reveals the coefficients of different independent variables, or driving factors, in predicting transition areas in LST. A positive and statistically significant correlation was observed between the transition area from NDBI, NDBAI, BSI, and SAVI to LST, indicating a link between urbanization, NDVI, MSI, NDWI, MNDWI, and LST changes. Conversely, this research identified a negative correlation with LST, signifying the inverse relationship among the LST and the geophysical indicators under consideration. There is a complex interplay between LST dynamics and the complex dimensions of physical parameters. By employing Spearman's correlation, this study transcended mere statistical analysis, delving into the intricate nuances of environmental interactions, as detailed in Table 7.

A better comprehension of that complex relationship is enhanced by such result between ecological parameters and LST dynamics, having consequences for the development of land use and the implementation of environmental ways of managing. The correlation analysis unveiled complex associations between LST and various geophysical indices, shedding light on the intricate dynamics governing thermal patterns. Notably, LST showed a favorable correlation with (BSI) (r = 0.417) and SAVI (r = 0.571), underscoring their influence on temperature dynamics.

Furthermore, a lower but evident significant connection was found between LST and NDBI (r = 0.235), as well as NDBAI (r = 0.388). Conversely, MNDWI, NDVI, SAVI, and NDWI displayed negative correlations with LST. These findings elucidate the complex relationships between LST and geophysical parameters, providing valuable insights into the complex interplay shaping thermal environments. To cope with the rapid temperature of the influence exerted by ecological parameters on LST within the broader scope of environmental research, particularly within the realms of ecological analyses, this research highlighted the importance of evaluation and profound understanding of dynamic processes. By directing attention to rapidly expanding regions, the formulation of

well-informed policies within the area facilitated progress toward the adoption of more sustainable environmental practices.

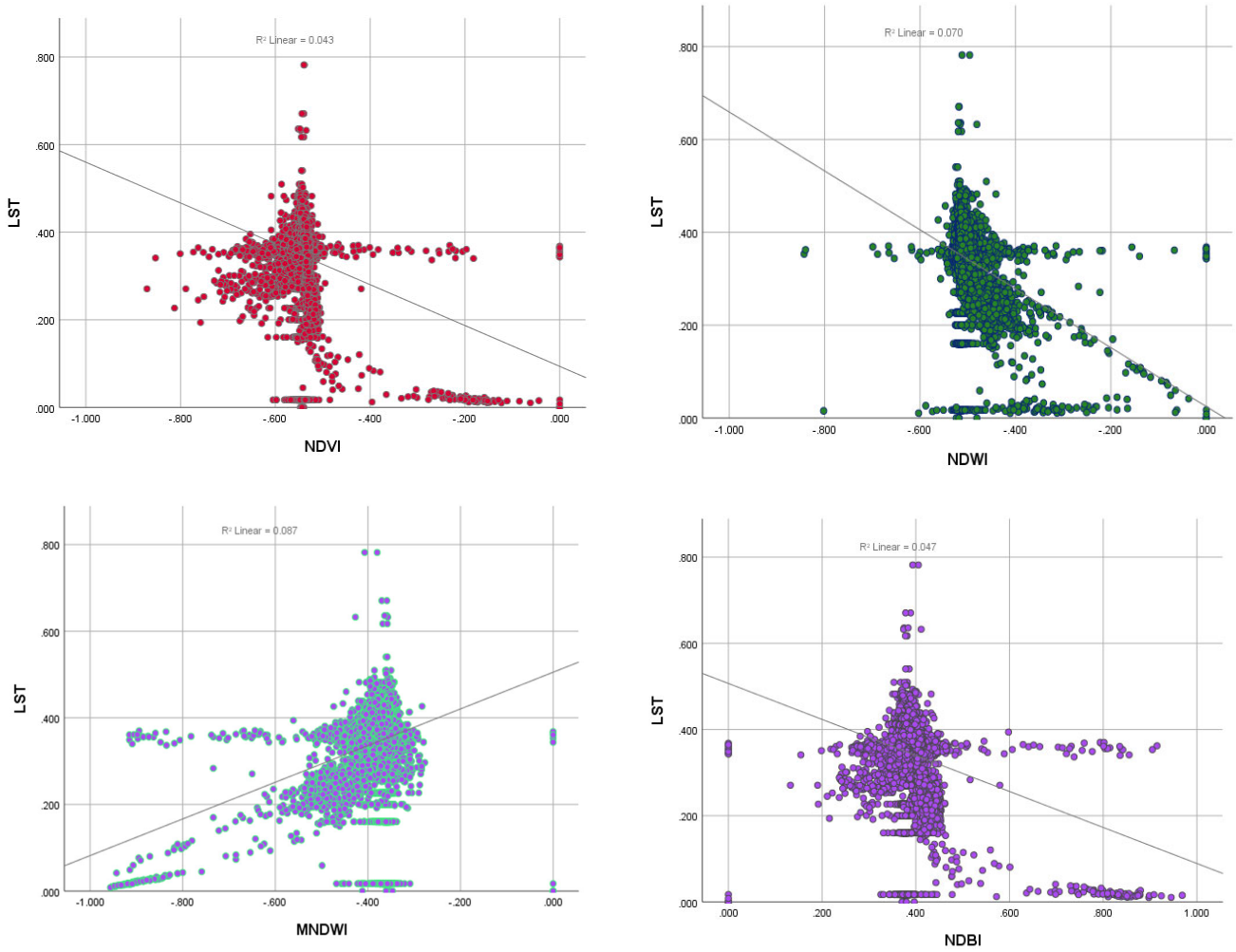

Figure 11. Scatter plot of the correlation between LST and the spatial indices (red color: NDVI vs. LST, green color: NDWI vs. LST, blue color: MNDWI vs. LST, magenta color: NDBI vs. LST).

Table 7. Correlation between the spatial indices and LST.

Biophysical Index	LST	NDVI	NDWI	NDBI	MNDWI	SAVI	MSI	NDBAI	BSI
LST	1	0.671 *	−0.288	0.538	−0.517	0.572	−0.198	0.288	0.474
NDVI	0.671 *	1	0.072	0.786 **	−0.032	0.544	0.293	0.193	0.808 **
NDWI	−0.288	0.072	1	−0.009	0.598	−0.295	−0.117	−0.600	0.223
NDBI	0.538	0.786 **	−0.009	1	−0.181	0.564	0.126	0.256	0.652 *
MNDWI	−0.517	−0.032	0.598	−0.181	1	−0.422	0.587	−0.722 *	0.178
SAVI	0.572	0.544	−0.295	0.564	−0.422	1	0.063	0.595	0.022
MSI	−0.198	0.293	−0.117	0.126	0.587	0.063	1	−0.177	0.215
NDBAI	0.288	0.193	−0.600	0.256	−0.722 *	0.595	−0.177	1	−0.077
BSI	0.474	0.808 **	0.223	0.652 *	0.178	0.022	0.215	−0.077	1

* Correlation is statistically significant at the 0.05 level (two-tailed). ** The Pearson correlation is significant at the 0.01 level (two-tailed).

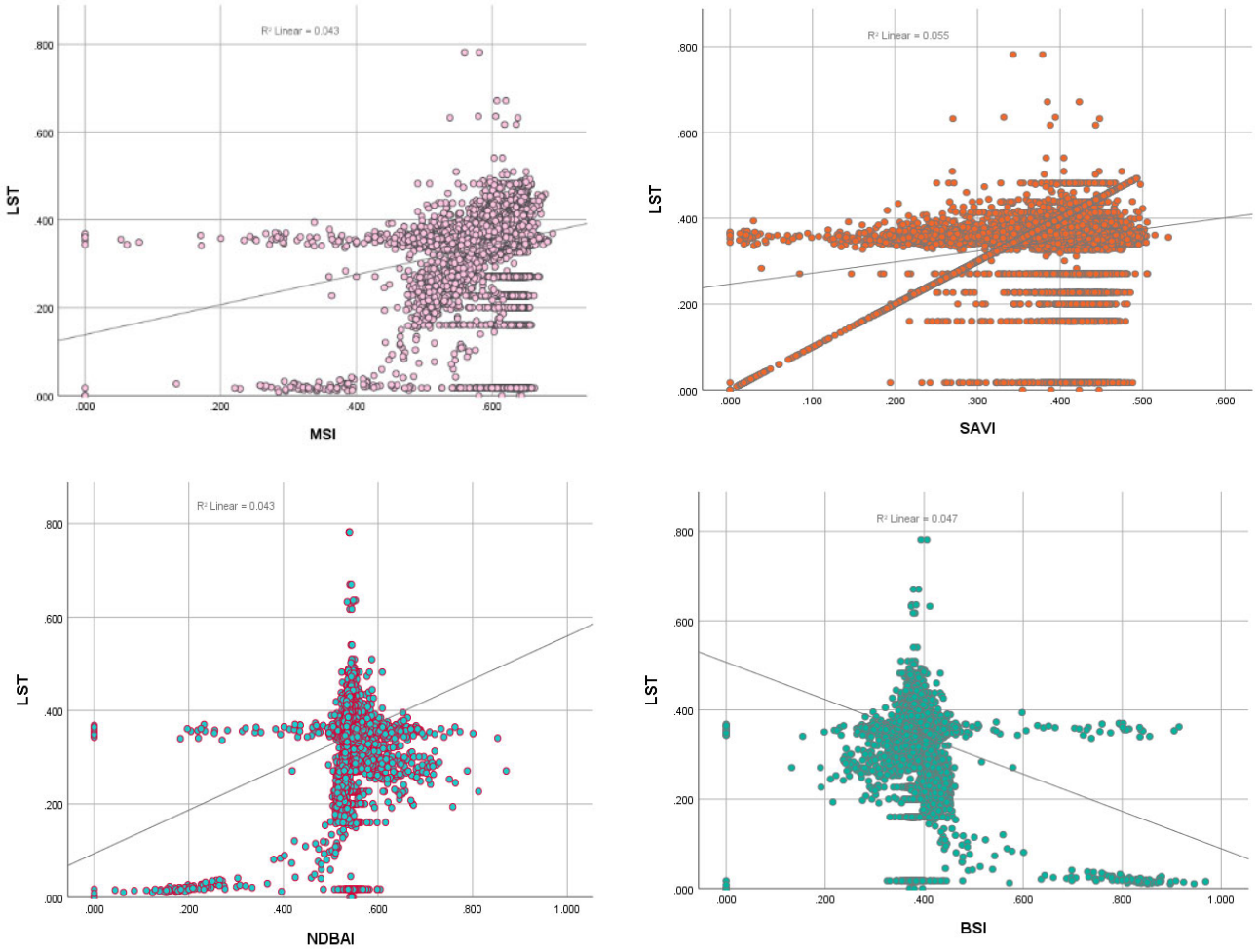

Figure 12. Scatter plot of the correlation between LST and spatial indices (reddish color: MSI vs. LST, orange color: SAVI vs. LST, red-blue color: NDBAI vs. LST, sky-blue color: BSI vs. LST).

3.6. Variables That Impact LST

This study also utilized the PCA technique to investigate the underlying factors influencing LST variations across the Dhaka, Gazipur, and Narayangonj districts (Table 8). The results revealed that Factor 1, which accounted for 60.82% of the total variance, were characterized by the interaction of NDWI and NDVI, reflecting water resources and vegetation cover. These factors emerged as crucial drivers of LST dynamics within urban settings. Previous studies consistently emphasized the inverse connection within the amount of greenery and LST, underlining the importance of vegetation areas and surface water sources in mitigating the heat of urban areas. Additionally, Factor 2, explaining 20.49% of the variance and dominated by SAVI and MSI associated with decreasing water body areas, highlighted the impact of human activities on LST. The existing literature affirmed that areas with extensive impervious surfaces tend to experience higher LST levels, which was explained 10.84% by Factor 3 containing NDBI and NDBAI. Together, these six factors elucidated over 80% of the total variance, providing valuable insights into the complex drivers of LST dynamics across the study area.

This study offers valuable insights into how the ecological development of three districts aligns with the principles of sustainable cities and communities. Also, the environmental susceptibility to potential consequences was actively quantified, which is caused by the changing patterns of LULC and environmental parameters over the Dhaka, Gazipur, and Narayangonj districts, spanning 1993 to 2023. The findings underscore a substantial linkage between the identified phenomena of the geophysical factors affecting LST and environmental sustainability.

Table 8. Principal component analysis of the factors.

Spatial Index	Principal Component				
	1	**2**	**3**	**4**	**5**
NDVI	**0.442**	−0.208	0.359	−0.501	−0.476
NDWI	**0.377**	−0.283	−0.175	−0.273	0.275
NDBI	−0.342	0.144	**0.440**	−0.283	0.200
MNDWI	0.262	−0.268	−0.370	0.206	**0.396**
SAVI	0.426	**0.604**	0.074	0.350	0.004
MSI	0.344	**0.347**	0.215	0.126	−0.040
NDBAI	0.262	−0.493	**0.531**	0.497	0.188
BSI	0.179	−0.235	−0.503	**0.408**	−0.681
Eigen Value	0.0082	0.0027	0.0014	0.0007	0.0002
Variance explained (%)	60.82	20.49	10.84	5.76	2.09
Cumulative (%)	60.82	81.31	92.15	97.91	100

4. Discussion

This study considered a detail investigation in exploring the relationship between urban expansion and environmental dynamics, focusing on the effect of ecological changes in rapidly growing urban areas. We found a direct relationship between LST and a declining trend of green spaces in the last 30 years in the study area. This was accompanied by a number of growing built-up areas and declining farmlands and water bodies. These changes had a profound impact on local climate, particularly deteriorating the urban temperature. Previous research showed that the loss of urban green spaces could lead to a 2–5 °C increase in LST due to reduced shading and evapotranspiration, while the absence of water bodies exacerbated this effect by diminishing evaporative cooling, resulting in up to 3 °C higher temperatures in surrounding areas [70]. Notably, our findings revealed that the 2.6 °C increase in LST in Dhaka, Gazipur, and Narayanganj over the past 30 years corresponded to a significant reduction in vegetation and water bodies.

A complex link between LST and several biophysical parameters has also been identified with a significantly strong association between LST and built-up areas (represented by BSI and SAVI), highlighting the significance of urban material in capturing and releasing the heat in raising the local temperature. Conversely, the negative relationship between LST and land covers (represented by NDVI and NDWI) indicates a reduction in heat absorption capacity through the natural cooling process. This strongly suggests the requirements of green urban infrastructures such as urban parks, green roofs, and water bodies, which can serve as effective mitigation strategies of adverse impacts of urbanization on local climate. This has been echoed in Bangladesh's National Urban Sector Policy and Dhaka Structure Plan 2016–2035 [71–73], which emphasizes that sustainable infrastructure and green urban spaces are critical. Furthermore, the connection between LST and physiological indices provides information to urban planners and policymakers for adopting environmentally friendly land use practices in the long run, which can significantly alleviate UHI effects, thereby improving urban environmental quality and residents' well-being.

Addressing the issues of ecological attributes with growing urbanization and climate change requires comprehensive analysis that includes adaptive ecological sustainability and environmental resiliency. This study underscores the importance of leveraging remote sensing and GIS technologies for monitoring urban environmental changes for ensuring a balance between development and ecology.

- The research reveals a strong association between alterations in vegetation cover and the dynamics of climate change within the study regions. A notable correlation between air temperature and the temporal shifts, suggesting a consistent trend toward rising temperatures [74], highlighting the anticipated changes in climatic conditions and ecological stability in the future.

- By exploring the degree of interplay between biophysical factors, a clear understanding of the evolving dynamics of region's ecosystem has been established. This in-depth examination provides a foundation for forecasting potential future urban development strategies.
- Throughout the period from 1993 to 2023, parameters, including NDVI, MSI, NDWI, and MNDWI, exhibited significant fluctuations, predominantly demonstrating an overall upward trend. Similarly, vegetation cover, as measured by the NDVI and SAVI indices, experienced fluctuations, particularly notable at the onset of the study period, with a slight inclination towards increase over time. Moreover, the statistical association between NDWI and MNDWI with climatic parameters surpassed that of NDBI, albeit marginally. This means that the study area underwent significant changes and might require immediate attention to retain sustainability.
- The findings reveal a noteworthy and statistically significant connection between the shift of various indices like NDBI, NDBAI, BSI, and SAVI to LST, which are closely related to the air and soil temperatures [75]. This will indicate the issues related to ground water retention, and changing the cropping patters in the study area.
- The study highlights the critical need for meticulous monitoring and understanding the complex interplay between climate change and the dynamics of ecological systems. Gaining the insights of these complex relationships is essential for effectively guiding sustainable environmental management strategies and informing policymaking initiatives within the region harmonized with government documents [76].
- The observations from this study reveal a potential divergence in the developmental trajectories of the Dhaka and Gazipur regions, characterized by an increase in built-up areas. These findings prompt further discussion on the potential ecological consequences and implications for biodiversity conservation and urban planning strategies in these areas.

Note that scientific evidence suggests that there are options for an adaptive urban solution tailored to local ecological dynamics [77]. Additionally, studies should investigate the long-term urban expansion on LST while incorporating climate modeling techniques. By aligning urban development with ecological sustainability, these efforts will contribute to the creation of a temperature friendly and more livable urban environment. In South Asia, integrating NBSs (nature-based solutions) with tools like GIS and GEE can help prioritize ecologically sensitive areas. By combining green infrastructure with digital planning technologies, cities can align urban growth to achieve environmental sustainability goals [78].

Furthermore, the ANOVA result revealed a F-statistic of 1.8549 and a p-value of 0.1906, indicating no significant differences in precision among the years. The F-statistic, reflecting the ratio of between-group variance to within-group variance, suggested that while variations exist, they were not statistically significant. The p-value exceeded the conventional significance threshold of 0.05, leading to the acceptance of the null hypothesis, which posited no significant differences in precision values over time. These findings implied consistent performance of the classification model, indicating reliability in LULC assessments across the years. The findings of this study highlight the significant influence of urbanization and ecological parameters on LST in the Dhaka, Gazipur, and Narayangonj districts. The correlations with biophysical indices, such as NDVI, SAVI, and BSI, indicated that reduced vegetation and increased impervious surfaces contributed to elevated temperatures in urban areas. To enhance the interpretation of these LST patterns, the integration of urban thermal comfort models, such as PALM, SOLWEIG, MITRAS, Rayman, and ENVI-met would be crucial.

For instance, ENVI-met [79] and PALM [80,81] could model microclimate dynamics within the identified UHI zones, illustrating how LST variations impacted human thermal comfort at a local level by accounting for factors like solar radiation and shading. These models would complement our findings by linking LST data with human-perceived temperatures, providing a more comprehensive understanding of thermal discomfort. Moreover, MITRAS model [82] could be applied to evaluate thermal stress in high-LST areas by simulating individual exposure to solar radiation and air temperature. The correlations

observed between LST and indices such as SAVI or BSI could be further interpreted through Rayman to assess how surface temperature increases exacerbate heat stress [83–85].

Finally, larger-scale models like COSMO [86] could integrate meteorological factors such as wind, humidity, and rainfall into the analysis, offering insights into how broader climatic conditions contributed to LST variability. While this study primarily focused on geophysical factors, incorporating thermal comfort models would provide a more holistic view of the interaction between LST and human thermal experiences, reinforcing the relevance of these findings for urban planning and sustainable development strategies.

Limitation and Future Research

This study highlighted the relationship between urbanization, environmental degradation, and the UHI effect, but several limitations must be acknowledged in future research. The primary challenge was the reliance on cloud-free satellite data, which limited the dataset, particularly in a tropical region like Bangladesh. While cloud masking techniques were applied, the data quality could still impact the accuracy of land use and land cover LULC classifications. Additionally, manual interpretation of satellite imagery introduced potential for human error, especially when distinguishing between similar land cover types such as vegetation and built-up areas. The 30 m spatial resolution of Landsat imagery also restricted the precision of the analysis, particularly in densely urbanized or heterogeneous areas. Future research could address these limitations by incorporating higher-resolution satellite data, such as Sentinel-2 or commercial platforms, which provided finer spatial details. Automated machine learning methods, such as convolutional neural networks (CNNs), could further improve classification accuracy by reducing manual errors and better capturing land-cover changes. Beyond surface temperature and LULC, future research should consider integrating additional environmental variables, such as air quality, humidity, and real-time ground-based sensor data. This would offer a more comprehensive view of urban environmental dynamics. Furthermore, exploring the socio-economic impacts of UHI and assessing mitigation strategies like green infrastructure could inform more sustainable urban planning practices.

5. Conclusions

Employing a combination of GIS and remotely sensed data tools, this research examined ecological trends, alterations to the landscape, and fluctuations in ground temperature in the Dhaka, Gazipur, and Narayanganj regions spanning 1993 to 2023. Through the analysis of multi-stage remote sensing data and spatial metrics, we delineated the complex interplay between urban expansion, environmental transformations, and their consequent effects on local climate. Consequently, we explored the influence of urban development (i.e., urban built-up areas) and water body reductions in LST changes during peak summer season. The results demonstrated that the temperature (i.e., LST) surpassed 36.52 °C in some heavily built-up areas.

Our findings revealed a prominent correlation between LST and biophysical indicators such as the BSI and SAVI, whereas weak relationships were observed with the NDBI and NDBAI. Conversely, MNDWI, MSI, NDVI, SAVI, and NDWI exhibited negative associations with LST. This underscored the intricate linkage between urbanization, ecological changes, and escalating surface temperatures, marking a trend toward rising urban heat. Moreover, the association of LST with NDVI and NDBI was found to be slightly positive, which demonstrated the influence of water bodies and natural resources on the positive trend of LST changes.

This research paper emphasizes the necessity of incorporating sustainable urban development and green infrastructure into urban planning. Our findings strongly emphasize the need to prioritize urban parks, green roofs, and water-sensitive urban designs to mitigate LST effectively. Additionally, restoring water bodies, enforcing sustainable zoning laws, and fostering public–private partnerships are essential to enhance green infrastructure. Aligning these strategies with national policies would not only mitigate UHI impacts, but also improve the quality of urban life and ensure long-term ecological resilience. The insights derived from this research might offer valuable guidance in order to promote secure

and habitable cityscapes in the areas with similar urban characteristics. By embracing these sustainable practices, cities could better adapt to the potential impacts of climate change. Of note, we recommend that researchers collect reliable datasets prior to adopting the methods applied in this research at other geographical locations.

Author Contributions: Conceptualization, M.T.M.; methodology M.T.M., J.N.F. and K.R.R.; Software: M.T.M., J.N.F., R.R. and K.R.R.; validation, M.T.M., J.N.F., P.K.J. and K.R.R.; formal analysis, M.T.M., J.N.F., R.R., J.H. and K.R.R.; investigation, M.T.M. and K.R.R.; resources, M.T.M., P.K.J., J.H. and K.R.R.; writing—original draft preparation, M.T.M., J.N.F., P.K.J., S.A.U. and, K.R.R.; writing—review and editing M.T.M., J.N.F., A.A.K., P.K.J., S.A.U., J.H. and K.R.R.; visualization, M.T.M., J.N.F., P.K.J. and K.R.R.; supervision: M.T.M. and K.R.R.; project administration M.T.M. and K.R.R.; funding acquisition, K.R.R. All authors have read and agreed to the published version of the manuscript.

Funding: The research project did not receive any funding.

Institutional Review Board Statement: Not applicable.

Informed Consent Statement: All participants were comprehensively briefed on the assurance of their anonymity, the purpose behind the research, and the potential utilization of the data in case of publication. As is standard in all research involving human subjects, ethical approval from the relevant ethics committee was secured.

Data Availability Statement: The data presented in this study are available on request. The data are not publicly available due to privacy.

Conflicts of Interest: The authors declare no conflicts of interest.

Appendix A

Table A1. Measurements for evaluating the models of the categorized data.

District	Year	Parameter	Built-Up	Waterbody	Barren Land	Vegetation	Accuracy	Macro Avg.	Weighted Avg.
Dhaka	1993	Accuracy	0.885	0.887	0.833	0.897	0.899	0.871	0.890
		Recall	0.893	0.869	0.759	0.865	0.899	0.873	0.809
		F1-score	0.949	0.893	0.795	0.881	0.899	0.891	0.898
		AUC	0.881	0.909	0.867	0.920			
	1999	Accuracy	0.867	0.865	0.965	0.967	0.868	0.894	0.868
		Recall	0.700	0.712	0.912	0.989	0.868	0.921	0.867
		F1-score	0.827	0.838	0.938	0.978	0.868	0.846	0.867
		AUC	0.883	0.852	0.952	0.990			
	2005	Accuracy	0.817	0.787	0.818	0.887	0.852	0.864	0.921
		Recall	0.752	0.869	0.750	0.869	0.852	0.863	0.922
		F1-score	0.835	0.793	0.783	0.878	0.852	0.868	0.921
		AUC	0.566	0.909	0.865	0.922			
	2011	Accuracy	0.548	0.864	0.905	0.893	0.893	0.927	0.840
		Recall	0.760	0.863	0.809	0.809	0.893	0.911	0.840
		F1-score	0.854	0.868	0.854	0.801	0.893	0.918	0.839
		AUC	0.870	0.868	0.900	0.840			
	2017	Accuracy	0.848	0.875	0.773	0.844	0.851	0.875	0.880
		Recall	0.803	0.854	0.680	0.835	0.851	0.854	0.871
		F1-score	0.860	0.874	0.723	0.840	0.851	0.864	0.860
		AUC	0.971	0.936	0.835	0.904			
	2023	Accuracy	0.844	0.929	0.833	0.739	0.891	0.861	0.904
		Recall	0.827	0.875	0.682	0.837	0.891	0.840	0.901
		F1-score	0.835	0.854	0.750	0.785	0.891	0.848	0.902
		AUC	0.842	0.864	0.838	0.892			

Table A1. *Cont.*

District	Year	Parameter	Built-Up	Waterbody	Barren Land	Vegetation	Accuracy	Macro Avg.	Weighted Avg.
Narayanganj	1993	Accuracy	0.875	0.884	0.837	0.864	0.857	0.853	0.877
		Recall	0.875	0.892	0.785	0.853	0.857	0.849	0.877
		F1-score	0.875	0.888	0.892	0.859	0.857	0.851	0.877
		AUC	0.935	0.885	0.887	0.872			
	1999	Accuracy	0.911	0.882	0.857	0.813	0.860	0.916	0.884
		Recall	0.898	0.833	0.837	0.925	0.860	0.898	0.880
		F1-score	0.905	0.857	0.785	0.865	0.860	0.891	0.897
		AUC	0.941	0.858	0.892	0.936			
	2005	Accuracy	0.883	0.833	0.844	0.897	0.907	0.926	0.938
		Recall	0.838	0.682	0.887	0.897	0.907	0.925	0.937
		F1-score	0.909	0.750	0.795	0.897	0.907	0.925	0.937
		AUC	0.848	0.838	0.842	0.939			
	2011	Accuracy	0.870	0.869	0.941	0.887	0.912	0.915	0.894
		Recall	0.920	0.848	0.864	0.907	0.912	0.910	0.892
		F1-score	0.895	0.858	0.901	0.893	0.912	0.912	0.892
		AUC	0.936	0.862	0.928	0.940			
	2017	Accuracy	0.920	0.833	0.868	0.845	0.848	0.898	0.909
		Recall	0.932	0.682	0.846	0.825	0.848	0.874	0.908
		F1-score	0.92	0.750	0.905	0.835	0.848	0.884	0.898
		AUC	0.948	0.838	0.864	0.898			
	2023	Accuracy	0.915	0.833	0.729	0.797	0.896	0.852	0.905
		Recall	0.928	0.882	0.729	0.763	0.896	0.847	0.906
		F1-score	0.891	0.850	0.729	0.780	0.896	0.850	0.905
		AUC	0.884	0.838	0.854	0.866			
Gazipur	1993	Accuracy	0.727	0.788	0.809	0.833	0.919	0.851	0.849
		Recall	0.571	0.879	0.809	0.882	0.919	0.835	0.849
		F1-score	0.640	0.884	0.809	0.850	0.919	0.840	0.848
		AUC	0.782	0.872	0.893	0.838			
	1999	Accuracy	0.811	0.877	0.837	0.857	0.878	0.896	0.850
		Recall	0.811	0.894	0.837	0.846	0.878	0.872	0.850
		F1-score	0.811	0.886	0.837	0.898	0.878	0.883	0.850
		AUC	0.897	0.866	0.910	0.920			
	2005	Accuracy	0.902	0.833	0.816	0.825	0.877	0.869	0.858
		Recall	0.881	0.782	0.889	0.854	0.877	0.865	0.857
		F1-score	0.892	0.850	0.851	0.839	0.877	0.866	0.857
		AUC	0.935	0.838	0.934	0.870			
	2011	Accuracy	0.905	0.973	0.837	0.950	0.858	0.916	0.848
		Recall	0.962	0.888	0.783	0.851	0.858	0.896	0.848
		F1-score	0.933	0.881	0.809	0.898	0.858	0.905	0.848
		AUC	0.872	0.870	0.883	0.922			
	2017	Accuracy	0.871	0.873	0.840	0.819	0.839	0.888	0.929
		Recall	0.921	0.869	0.750	0.908	0.839	0.887	0.929
		F1-score	0.821	0.871	0.792	0.861	0.839	0.886	0.928
		AUC	0.953	0.864	0.865	0.938			
	2023	Accuracy	0.905	0.867	0.682	0.776	0.873	0.832	0.908
		Recall	0.934	0.882	0.341	0.868	0.873	0.781	0.913
		F1-score	0.899	0.874	0.455	0.819	0.873	0.792	0.907
		AUC	0.836	0.876	0.665	0.920			

References

1. Choudhury, D.; Das, K.; Das, A. Assessment of land use land cover changes and its impact on variations of land surface temperature in Asansol-Durgapur Development Region. *Egypt. J. Remote Sens. Space Sci.* **2019**, *22*, 203–218. [CrossRef]
2. Sannigrahi, S.; Bhatt, S.; Rahmat, S.; Uniyal, B.; Banerjee, S.; Chakraborti, S.; Jha, S.; Lahiri, S.; Santra, K.; Bhatt, A. Analyzing the role of biophysical compositions in minimizing urban land surface temperature and urban heating. *Urban Clim.* **2018**, *24*, 803–819. [CrossRef]
3. Al Kafy, A.; Faisal, A.A.; Sikdar, S.; Hasan, M.; Rahman, M.; Khan, M.H.; Islam, R. Impact of LULC Changes on LST in Rajshahi District of Bangladesh: A Remote Sensing Approach. *J. Geogr. Stud.* **2020**, *3*, 11–23. [CrossRef]
4. Koko, A.F.; Wu, Y.; Abubakar, G.A.; Alabsi, A.A.N.; Hamed, R.; Bello, M. Thirty Years of Land Use/Land Cover Changes and Their Impact on Urban Climate: A Study of Kano Metropolis, Nigeria. *Land* **2021**, *10*, 1106. [CrossRef]
5. Addas, A. Understanding the Relationship between Urban Biophysical Composition and Land Surface Temperature in a Hot Desert Megacity (Saudi Arabia). *Int. J. Environ. Res. Public Health* **2023**, *20*, 5025. [CrossRef]
6. Mukherjee, F.; Singh, D. Assessing Land Use–Land Cover Change and Its Impact on Land Surface Temperature Using LANDSAT Data: A Comparison of Two Urban Areas in India. *Earth Syst. Environ.* **2020**, *4*, 385–407. [CrossRef]
7. Yan, Z.; Teng, M.; He, W.; Liu, A.; Li, Y.; Wang, P. Impervious surface area is a key predictor for urban plant diversity in a city undergone rapid urbanization. *Sci. Total Environ.* **2019**, *650*, 335–342. [CrossRef]
8. Salerno, F.; Viviano, G.; Tartari, G. Urbanization and climate change impacts on surface water quality: Enhancing the resilience by reducing impervious surfaces. *Water Res.* **2018**, *144*, 491–502. [CrossRef]
9. Zhang, J.; Jiao, G.; Ye, Q.; Gu, X. The Impact of Urban Expansion on the Urban Thermal Environment: A Case Study in Nanchang, Jiangxi, China. *Sustainability* **2022**, *14*, 16531. [CrossRef]
10. Du, J.; Xiang, X.; Zhao, B.; Zhou, H. Impact of urban expansion on land surface temperature in Fuzhou, China using Landsat imagery. *Sustain. Cities Soc.* **2020**, *61*, 102346. [CrossRef]
11. Siqi, J.; Yuhong, W. Effects of land use and land cover pattern on urban temperature variations: A case study in Hong Kong. *Urban Clim.* **2020**, *34*, 100693. [CrossRef]
12. Mallick, J.; Alsubih, M.; Ahmed, M.; Almesfer, M.K.; Kahla, N.B. Assessing the Spatiotemporal Heterogeneity of Terrestrial Temperature as a Proxy to Microclimate and Its Relationship with Urban Hydro-Biophysical Parameters. *Front. Ecol. Evol.* **2022**, *10*, 878375. [CrossRef]
13. Macarof, P.; Statescu, F. Comparasion of NDBI and NDVI as Indicators of Surface Urban Heat Island Effect in Landsat 8 Imagery: A Case Study of Iasi. *Present Environ. Sustain. Dev.* **2017**, *11*, 141–150. [CrossRef]
14. Zhang, T.; Huang, X. Monitoring of Urban Impervious Surfaces Using Time Series of High-Resolution Remote Sensing Images in Rapidly Urbanized Areas: A Case Study of Shenzhen. *IEEE J. Sel. Top. Appl. Earth Obs. Remote Sens.* **2018**, *11*, 2692–2708. [CrossRef]
15. Firozjaei, M.K.; Alavipanah, S.K.; Liu, H.; Sedighi, A.; Mijani, N.; Kiavarz, M.; Weng, Q. A PCA-OLS model for assessing the impact of surface biophysical parameters on land surface temperature variations. *Remote Sens.* **2019**, *11*, 2094. [CrossRef]
16. Small, C. Comparative analysis of urban reflectance and surface temperature. *Remote Sens. Environ.* **2006**, *104*, 168–189. [CrossRef]
17. Abu, A.; Fauzi, R. Land Surface Temperature and Biophysical Factors in Urban Planning. 2014. Available online: https://www.researchgate.net/publication/232273165 (accessed on 17 May 2014).
18. Obiakor, M.; Ezeonyejiaku, C.D.; Mogbo, T.C. Effects of Vegetated and Synthetic (Impervious) Surfaces on the Microclimate of Urban Area. *J. Appl. Sci. Environ. Manag.* **2012**, *16*, 85–94. Available online: www.bioline.org.br/ja (accessed on 15 July 2013).
19. Li, L.; Wang, Y.; Liu, C. Effects of land use changes on soil erosion in a fast developing area. *Int. J. Environ. Sci. Technol.* **2014**, *11*, 1549–1562. [CrossRef]
20. Azhdari, A.; Soltani, A.; Alidadi, M. Urban morphology and landscape structure effect on land surface temperature: Evidence from Shiraz, a semi-arid city. *Sustain. Cities Soc.* **2018**, *41*, 853–864. [CrossRef]
21. Imran, H.M.; Hossain, A.; Islam, A.S.; Rahman, A.; Bhuiyan, M.A.E.; Paul, S.; Alam, A. Impact of Land Cover Changes on Land Surface Temperature and Human Thermal Comfort in Dhaka City of Bangladesh. *Earth Syst. Environ.* **2021**, *5*, 667–693. [CrossRef]
22. Zhang, Q.; Wu, Z.; Yu, H.; Zhu, X.; Shen, Z. Variable Urbanization Warming Effects across Metropolitans of China and Relevant Driving Factors. *Remote Sens.* **2020**, *12*, 1500. [CrossRef]
23. Liu, Y.; Peng, J.; Wang, Y. Efficiency of landscape metrics characterizing urban land surface temperature. *Landsc. Urban Plan.* **2018**, *180*, 36–53. [CrossRef]
24. Estoque, R.C.; Murayama, Y.; Myint, S.W. Effects of landscape composition and pattern on land surface temperature: An urban heat island study in the megacities of Southeast Asia. *Sci. Total Environ.* **2017**, *577*, 349–359. [CrossRef] [PubMed]
25. Mathew, A.; Khandelwal, S.; Kaul, N. Spatial and temporal variations of urban heat island effect and the effect of percentage impervious surface area and elevation on land surface temperature: Study of Chandigarh city, India. *Sustain. Cities Soc.* **2016**, *26*, 264–277. [CrossRef]
26. Pathak, C.; Chandra, S.; Maurya, G.; Rathore, A.; Sarif, M.O.; Gupta, R.D. The Effects of Land Indices on Thermal State in Surface Urban Heat Island Formation: A Case Study on Agra City in India Using Remote Sensing Data (1992–2019). *Earth Syst. Environ.* **2021**, *5*, 135–154. [CrossRef]

27. Roy, B.; Bari, E.; Nipa, N.J.; Ani, S.A. Comparison of temporal changes in urban settlements and land surface temperature in Rangpur and Gazipur Sadar, Bangladesh after the establishment of city corporation. *Remote Sens. Appl.* **2021**, *23*, 100587. [CrossRef]
28. Abdullah, H.M.; Islam, I.; Miah, M.G.; Ahmed, Z. Quantifying the spatiotemporal patterns of forest degradation in a fragmented, rapidly urbanizing landscape: A case study of Gazipur, Bangladesh. *Remote Sens. Appl.* **2019**, *13*, 457–465. [CrossRef]
29. Hossain, M.A.; Huggins, R. The Environmental and Social Impacts of Unplanned and Rapid Industrialization in Suburban Areas: The Case of the Greater Dhaka Region, Bangladesh. *Environ. Urban. ASIA* **2021**, *12*, 73–89. [CrossRef]
30. Karimi, A.; Mohammad, P.; García-Martínez, A.; Moreno-Rangel, D.; Gachkar, D.; Gachkar, S. New developments and future challenges in reducing and controlling heat island effect in urban areas. *Environ. Dev. Sustain.* **2023**, *25*, 10485–10531. [CrossRef]
31. Rana, M.M.; Sulaiman, N.; Sivertsen, B.; Khan, M.F.; Nasreen, S. Trends in atmospheric particulate matter in Dhaka, Bangladesh, and the vicinity. *Environ. Sci. Pollut. Res.* **2016**, *23*, 17393–17403. [CrossRef]
32. Miah, M.T.; Fariha, J.N.; Kafy, A.A.; Islam, R.; Biswas, N.; Duti, B.M.; Fattah, A.; Alsulamy, S.; Khedher, K.M.; Salem, M.A. Exploring the nexus between land cover change dynamics and spatial heterogeneity of demographic trajectories in rapidly growing ecosystems of south Asian cities. *Ecol. Indic.* **2024**, *158*, 111299. [CrossRef]
33. Hassan, M.; Southworth, J. Analyzing Land Cover Change and Urban Growth Trajectories of the Mega-Urban Region of Dhaka Using Remotely Sensed Data and an Ensemble Classifier. *Sustainability* **2017**, *10*, 10. [CrossRef]
34. Faisal, A.-A.; Al Kafy, A.; Al Rakib, A.; Akter, K.S.; Jahir, D.M.A.; Sikdar, M.S.; Ashrafi, T.J.; Mallik, S.; Rahman, M. Assessing and predicting land use/land cover, land surface temperature and urban thermal field variance index using Landsat imagery for Dhaka Metropolitan area. *Environ. Chall.* **2021**, *4*, 100192. [CrossRef]
35. BBS. Statistics and Informatics Division (Sid) Ministry of Planning, Government of the People's Republic of Bangladesh. In *Bangladesh Bureau of Statistics (BBS).*; 2013. Available online: http://nsds.bbs.gov.bd/en (accessed on 24 October 2024).
36. Rashid, N.; Alam, J.A.M.M.; Chowdhury, M.A.; Islam, S.L.U. Impact of landuse change and urbanization on urban heat island effect in Narayanganj city, Bangladesh: A remote sensing-based estimation. *Environ. Chall.* **2022**, *8*, 100571. [CrossRef]
37. Noman, A.H.M.; Mia, M.A.; Banna, H.; Rana, M.S.; Alam, A.F.; Gee, C.S.; Isa, C.R.; Er, A.C. City profile: Narayanganj, Bangladesh. *Cities* **2016**, *59*, 8–19. [CrossRef]
38. Guttikunda, S.K.; Begum, B.A.; Wadud, Z. Particulate pollution from brick kiln clusters in the Greater Dhaka region, Bangladesh. *Air Qual. Atmos. Health* **2013**, *6*, 357–365. [CrossRef]
39. Morshed, N.; Yorke, C.; Zhang, Q. Urban Expansion Pattern and Land Use Dynamics in Dhaka, 1989–2014. *Prof. Geogr.* **2017**, *69*, 396–411. [CrossRef]
40. Fariha, J.N.; Miah, M.T.; Limon, Z.A.; Alsulamy, S.; Al Kafy, A.; Rahman, S.N. Quantifying spatial dynamics of urban sprawl for climate resilience sustainable natural resource management by utilizing geostatistical and remote sensing techniques. *Theor. Appl. Clim.* **2024**, *155*, 6307–6349. [CrossRef]
41. Arifeen, H.M.; Phoungthong, K.; Mostafaeipour, A.; Yuangyai, N.; Yuangyai, C.; Techato, K.; Jutidamrongphan, W. Determine the Land-Use Land-Cover Changes, Urban Expansion and Their Driving Factors for Sustainable Development in Gazipur Bangladesh. *Atmosphere* **2021**, *12*, 1353. [CrossRef]
42. Naibbi, A.I.; Baily, B.; Healey, R.G.; Collier, P. Changing Vegetation Patterns in Yobe State Nigeria: An Analysis of the Rates of Change, Potential Causes and the Implications for Sustainable Resource Management. *Int. J. Geosci.* **2014**, *05*, 50–62. [CrossRef]
43. Warrens, M.J. Five Ways to Look at Cohens Kappa. *J. Psychol. Psychother.* **2015**, *5*, 4. [CrossRef]
44. de Mast, J. Agreement and Kappa-Type Indices. *Am. Stat.* **2007**, *61*, 148–153. [CrossRef]
45. Foody, G.M. Explaining the unsuitability of the kappa coefficient in the assessment and comparison of the accuracy of thematic maps obtained by image classification. *Remote Sens. Environ.* **2020**, *239*, 111630. [CrossRef]
46. Tassi, A.; Vizzari, M. Object-Oriented LULC Classification in Google Earth Engine Combining SNIC, GLCM, and Machine Learning Algorithms. *Remote Sens.* **2020**, *12*, 3776. [CrossRef]
47. Stehman, S.V. Selecting and interpreting measures of thematic classification accuracy. *Remote Sens. Environ.* **1997**, *62*, 77–89. [CrossRef]
48. Tsutsumida, N.; Comber, A.J. Measures of spatio-temporal accuracy for time series land cover data. *Int. J. Appl. Earth Obs. Geoinf.* **2015**, *41*, 46–55. [CrossRef]
49. Heagerty, P.J.; Lumley, T.; Pepe, M.S. Time-Dependent ROC Curves for Censored Survival Data and a Diagnostic Marker. *Biometrics* **2000**, *56*, 337–344. [CrossRef]
50. Walter, S.D. The partial area under the summary ROC curve. *Stat. Med.* **2005**, *24*, 2025–2040. [CrossRef] [PubMed]
51. Kumar, D.; Pfeiffer, M.; Gaillard, C.; Langan, L.; Scheiter, S. Climate change and elevated CO2 favor forest over savanna under different future scenarios in South Asia. *Biogeosciences* **2021**, *18*, 2957–2979. [CrossRef]
52. Ullah, S.; Ahmad, K.; Sajjad, R.U.; Abbasi, A.M.; Nazeer, A.; Tahir, A.A. Analysis and simulation of land cover changes and their impacts on land surface temperature in a lower Himalayan region. *J. Environ. Manag.* **2019**, *245*, 348–357. [CrossRef]
53. Zhu, X.; Wang, X.; Yan, D.; Liu, Z.; Zhou, Y. Analysis of remotely-sensed ecological indexes' influence on urban thermal environment dynamic using an integrated ecological index: A case study of Xi'an, China. *Int. J. Remote Sens.* **2019**, *40*, 3421–3447. [CrossRef]
54. Abutaleb, K.; Ngie, A.; Darwish, A.; Ahmed, M.; Arafat, S.; Ahmed, F. Assessment of Urban Heat Island Using Remotely Sensed Imagery over Greater Cairo, Egypt. *Adv. Remote Sens.* **2015**, *4*, 35–47. [CrossRef]

55. Gascon, M.; Cirach, M.; Martínez, D.; Dadvand, P.; Valentín, A.; Plasència, A.; Nieuwenhuijsen, M.J. Normalized difference vegetation index (NDVI) as a marker of surrounding greenness in epidemiological studies: The case of Barcelona city. *Urban. Urban. Green.* **2016**, *19*, 88–94. [CrossRef]
56. Özelkan, E. Water body detection analysis using NDWI indices derived from landsat-8 OLI. *Pol. J. Environ. Stud.* **2020**, *29*, 1759–1769. [CrossRef]
57. Arekhi, M.; Goksel, C.; Sanli, F.B.; Senel, G. Comparative evaluation of the spectral and spatial consistency of Sentinel-2 and Landsat-8 OLI data for Igneada longos forest. *ISPRS Int. J. Geoinf.* **2019**, *8*, 56. [CrossRef]
58. Mfondoum, A.H.N.; Etouna, J.; Nongsi, B.K.; Moto, F.A.M.; Deussieu, F.G.N. Assessment of Land Degradation Status and Its Impact in Arid and Semi-Arid Areas by Correlating Spectral and Principal Component Analysis Neo-Bands. *Int. J. Adv. Remote Sens. GIS* **2016**, *5*, 1539–1560. [CrossRef]
59. Wang, Y.; Zhan, Q.; Ouyang, W. How to quantify the relationship between spatial distribution of urban waterbodies and land surface temperature? *Sci. Total Environ.* **2019**, *671*, 1–9. [CrossRef]
60. Nguyen, C.T.; Chidthaisong, A.; Diem, P.K.; Huo, L.-Z. A Modified Bare Soil Index to Identify Bare Land Features during Agricultural Fallow-Period in Southeast Asia Using Landsat 8. *Land* **2021**, *10*, 231. [CrossRef]
61. Ren, H.; Zhou, G.; Zhang, F. Using negative soil adjustment factor in soil-adjusted vegetation index (SAVI) for aboveground living biomass estimation in arid grasslands. *Remote Sens. Environ.* **2018**, *209*, 439–445. [CrossRef]
62. Hong, Z.; Zhang, W.; Yu, C.; Zhang, D.; Li, L.; Meng, L. SWCTI: Surface Water Content Temperature Index for Assessment of Surface Soil Moisture Status. *Sensors* **2018**, *18*, 2875. [CrossRef]
63. Gelman, A. Analysis of variance—Why it is more important than ever. *Ann. Stat.* **2005**, *33*, 1–53. [CrossRef]
64. Asgarian, A.; Amiri, B.J.; Sakieh, Y. Assessing the effect of green cover spatial patterns on urban land surface temperature using landscape metrics approach. *Urban. Ecosyst.* **2015**, *18*, 209–222. [CrossRef]
65. Obilor, E.I.; Amadi, E.C. Test for Significance of Pearson's Correlation Coefficient. *Int. J. Innov. Math. Stat. Energy Policies* **2018**, *6*, 11–23.
66. Abdi, H.; Williams, L.J. Principal component analysis. *WIREs Comput. Stat.* **2010**, *2*, 433–459. [CrossRef]
67. Gohain, K.J.; Mohammad, P.; Goswami, A. Assessing the impact of land use land cover changes on land surface temperature over Pune city, India. *Quat. Int.* **2021**, *575–576*, 259–269. [CrossRef]
68. Santer, B.D.; Po-Chedley, S.; Zelinka, M.D.; Cvijanovic, I.; Bonfils, C.; Durack, P.J.; Fu, Q.; Kiehl, J.; Mears, C.; Painter, J.; et al. Human influence on the seasonal cycle of tropospheric temperature. *Science* **2018**, *361*, eaas8806. [CrossRef]
69. Guo, G.; Wu, Z.; Xiao, R.; Chen, Y.; Liu, X.; Zhang, X. Impacts of urban biophysical composition on land surface temperature in urban heat island clusters. *Landsc. Urban Plan.* **2015**, *135*, 1–10. [CrossRef]
70. Jandaghian, Z.; Colombo, A. The Role of Water Bodies in Climate Regulation: Insights from Recent Studies on Urban Heat Island Mitigation. *Buildings* **2024**, *14*, 2945. [CrossRef]
71. Roy, M. Planning for sustainable urbanisation in fast growing cities: Mitigation and adaptation issues addressed in Dhaka, Bangladesh. *Habitat. Int.* **2009**, *33*, 276–286. [CrossRef]
72. Smith, A.C.; Tasnim, T.; Irfanullah, H.M.; Turner, B.; Chausson, A.; Seddon, N. Nature-based Solutions in Bangladesh: Evidence of Effectiveness for Addressing Climate Change and Other Sustainable Development Goals. *Front. Environ. Sci.* **2021**, *9*, 737659. [CrossRef]
73. Zinia, N.J.; McShane, P. Ecosystem services management: An evaluation of green adaptations for urban development in Dhaka, Bangladesh. *Landsc. Urban Plan.* **2018**, *173*, 23–32. [CrossRef]
74. Cao, J.; Zhou, W.; Zheng, Z.; Ren, T.; Wang, W. Within-city spatial and temporal heterogeneity of air temperature and its relationship with land surface temperature. *Landsc. Urban. Plan.* **2021**, *206*, 103979. [CrossRef]
75. Stevens-Rumann, C.S.; Kemp, K.B.; Higuera, P.E.; Harvey, B.J.; Rother, M.T.; Donato, D.C.; Morgan, P.; Veblen, T.T. Evidence for declining forest resilience to wildfires under climate change. *Ecol. Lett.* **2018**, *21*, 243–252. [CrossRef]
76. Margerum, R.D.; Born, S.M. Integrated Environmental Management: Moving from Theory to Practice. *J. Environ. Plan. Manag.* **1995**, *38*, 371–392. [CrossRef]
77. Wu, Z.; Zhang, Y. Water Bodies' Cooling Effects on Urban Land Daytime Surface Temperature: Ecosystem Service Reducing Heat Island Effect. *Sustainability* **2019**, *11*, 787. [CrossRef]
78. Li, C.; Lu, L.; Fu, Z.; Sun, R.; Pan, L.; Han, L.; Guo, H.; Li, Q. Diverse cooling effects of green space on urban heat island in tropical megacities. *Front. Environ. Sci.* **2022**, *10*, 1073914. [CrossRef]
79. Bruse, M.; Fleer, H. Simulating surface–plant–air interactions inside urban environments with a three dimensional numerical model. *Environ. Model. Softw.* **1998**, *13*, 373–384. [CrossRef]
80. Anders, J.; Schubert, S.; Sauter, T.; Tunn, S.; Schneider, C.; Salim, M. Modelling the impact of an urban development project on microclimate and outdoor thermal comfort in a mid-latitude city. *Energy Build.* **2023**, *296*, 113324. [CrossRef]
81. Maronga, B.; Banzhaf, S.; Burmeister, C.; Esch, T.; Forkel, R.; Fröhlich, D.; Fuka, V.; Gehrke, K.F.; Geletič, J.; Giersch, S.; et al. Overview of the PALM model system 6.0. *Geosci. Model. Dev.* **2020**, *13*, 1335–1372. [CrossRef]
82. Salim, M.H.; Schlünzen, K.H.; Grawe, D.; Boettcher, M.; Gierisch, A.M.U.; Fock, B.H. The microscale obstacle-resolving meteorological model MITRAS v2.0: Model theory. *Geosci. Model. Dev.* **2018**, *11*, 3427–3445. [CrossRef]
83. Kumar, D.; Shekhar, S. Statistical analysis of land surface temperature–vegetation indexes relationship through thermal remote sensing. *Ecotoxicol. Environ. Saf.* **2015**, *121*, 39–44. [CrossRef] [PubMed]

84. Crank, P.J.; Middel, A.; Wagner, M.; Hoots, D.; Smith, M.; Brazel, A. Validation of seasonal mean radiant temperature simulations in hot arid urban climates. *Sci. Total Environ.* **2020**, *749*, 141392. [CrossRef] [PubMed]
85. Lee, H.; Mayer, H. Validation of the mean radiant temperature simulated by the RayMan software in urban environments. *Int. J. Biometeorol.* **2016**, *60*, 1775–1785. [CrossRef] [PubMed]
86. Baldauf, M.; Seifert, A.; Förstner, J.; Majewski, D.; Raschendorfer, M.; Reinhardt, T. Operational Convective-Scale Numerical Weather Prediction with the COSMO Model: Description and Sensitivities. *Mon. Weather. Rev.* **2011**, *139*, 3887–3905. [CrossRef]